# Longitudinal and transverse Greens functions in $\varphi^4$ model below and near the critical point

J. Kaupužs \*

Institute of Mathematics and Computer Science, University of Latvia 29 Rainja Boulevard, LV-1459 Riga, Latvia

October 28, 2018

#### Abstract

We have extended our method of grouping of Feynman diagrams (GFD theory) to study the transverse and longitudinal Greens functions  $G_{\perp}(\mathbf{k})$  and  $G_{\parallel}(\mathbf{k})$  in  $\varphi^4$  model below the critical point  $(T < T_c)$  in presence of an infinitesimal external field. Our method allows a qualitative analysis not cutting the perturbation series. We have shown that the critical behavior of the Greens functions is consistent with a general scaling hypothesis, where the same critical exponents, found within the GFD theory, are valid both at  $T < T_c$  and  $T > T_c$ . The long–wave limit  $k \to 0$  has been studied at  $T < T_c$ , showing that  $G_{\perp}(\mathbf{k}) \simeq a \, k^{-\lambda_{\perp}}$  and  $G_{\parallel}(\mathbf{k}) \simeq b \, k^{-\lambda_{\parallel}}$  with exponents  $d/2 < \lambda_{\perp} < 2$  and  $\lambda_{\parallel} = 2\lambda_{\perp} - d$  is the physical solution of our equations at the spatial dimensionality 2 < d < 4, which coincides with the asymptotic solution at  $T \to T_c$  as well as with a non–perturbative renormalization group (RG) analysis provided in our paper. It is confirmed also by Monte Carlo simulation. The exponents, as well as the ratio  $bM^2/a^2$  (where M is magnetization) are universal. The results of the perturbative RG method are reproduced by formally setting  $\lambda_{\perp} = 2$ . Nevertheless, we disprove the conventional statement that  $\lambda_{\perp} = 2$  is the exact result.

# 1 Introduction

Phase transitions and critical phenomena is a widely investigated field in physics and natural sciences [1, 2, 3, 4]. The current paper is devoted to further development of our original diagrammatic method introduced in [5], to study the  $\varphi^4$  phase transition model below the critical point. Our approach is based on a suitable grouping of Feynman diagrams, therefore we shall call it the GFD theory. In distinction to the conventional perturbative renormalization group (RG) method [3, 4], it allows a qualitative analysis near and at the critical point, not cutting the perturbation series. In such a way, we have found the set of possible values for exact critical exponents [5] in two and three dimensions in agreement with the known exact results for the two–dimensional Ising model [6, 7]. A good agreement with some Monte Carlo (MC) data [8, 9] and experiments [10] has been found in [5], as well. The disagreement with the conventionally accepted RG values of the critical exponents has been widely discussed in [11, 12], providing arguments that very sensitive numerical tests confirm our theoretical predictions.

<sup>\*</sup>E-mail: kaupuzs@latnet.lv

The  $\varphi^4$  model exhibits a nontrivial behavior in close vicinity, as well as below the critical temperature  $T_c$ , if the order parameter is an n-component vector with n > 1. The related long-wave divergence of the longitudinal and transverse correlation functions (in Fourier representation) at  $T < T_c$  has been studied in [13, 14] based on the hydrodynamical (Gaussian) approximation. Essentially the same problem has been studied before in [15] in terms of the Gaussian spin-wave theory [16]. Later perturbative renormalization group (RG) studies [17, 18, 19, 20, 21, 22, 23, 24, 25] support the Gaussian approximation. The RG method is claimed to be asymptotically exact. However, we disprove this statement by finding out the errors as well as unjustified assertions and assumptions in the papers where these claims have been established (Sec. 9.1). Our analysis predicts a non-Gaussian behavior, and we show by general physical arguments that it must be the true behavior to coincide with the know rigorous results for the classical XY model. This prediction is strongly supported by a Monte Carlo test (Sec. 10).

# 2 Primary equations

We consider a  $\varphi^4$  model with the Hamiltonian

$$H/T = \int \left( r_0 \varphi^2(\mathbf{x}) + c(\nabla \varphi(\mathbf{x}))^2 + u \varphi^4(\mathbf{x}) - \mathbf{h} \varphi(\mathbf{x}) \right) d\mathbf{x} , \qquad (1)$$

where the order parameter  $\varphi(\mathbf{x})$  is an *n*-component vector with components  $\varphi_i(\mathbf{x})$ , depending on the coordinate  $\mathbf{x}$ , T is the temperature,  $\mathbf{h}$  is an external field. The same model, but without the external field  $\mathbf{h}$ , has been discussed in [5], representing the  $\varphi^4$  term as

$$\int \int \varphi^{2}(\mathbf{x}_{1})u(\mathbf{x}_{1} - \mathbf{x}_{2})\varphi^{2}(\mathbf{x}_{2})d\mathbf{x}_{1}d\mathbf{x}_{2} 
= V^{-1} \sum_{i,j,\mathbf{k}_{1},\mathbf{k}_{2},\mathbf{k}_{3}} \varphi_{i}(\mathbf{k}_{1})\varphi_{i}(\mathbf{k}_{2})u_{\mathbf{k}_{1}+\mathbf{k}_{2}}\varphi_{j}(\mathbf{k}_{3})\varphi_{j}(-\mathbf{k}_{1} - \mathbf{k}_{2} - \mathbf{k}_{3}) ,$$
(2)

where in our special case of (1) we have  $u(\mathbf{x}) = \delta(\mathbf{x})$  and  $u_{\mathbf{k}} \equiv u$ . This is obtained by using the Fourier representation  $\varphi_i(\mathbf{x}) = V^{-1/2} \sum_{k < \Lambda} \varphi_i(\mathbf{k}) \, e^{i\mathbf{k}\mathbf{x}}$ , where  $V = L^d$  is the volume of the system and d is the spatial dimensionality. Like in [5], here we suppose that the field  $\varphi_i(\mathbf{x})$  does not contain the Fourier components  $\varphi_i(\mathbf{k})$  with  $k > \Lambda$ . At  $\mathbf{h} = \mathbf{0}$ , the model undergoes the second-order phase transition with a spontaneous long-range ordering. Besides, all the directions of ordering are equally probable. To remove this degeneracy, we consider the thermodynamic limit at an infinitesimal external field, i. e.,  $\lim_{h\to 0} \lim_{L\to\infty} \text{ where } h = |\mathbf{h}|$ . In this case the magnetization  $\mathbf{M} = \langle \varphi \rangle$  is oriented just along the external field. We consider also a model with Hamiltonian

$$H/T = \int \left( r_0 \varphi^2(\mathbf{x}) - \delta \cdot \varphi_1^2(\mathbf{x}) + c(\nabla \varphi(\mathbf{x}))^2 + u\varphi^4(\mathbf{x}) \right) d\mathbf{x} . \tag{3}$$

In the limit  $\lim_{\delta \to 0} \lim_{L \to \infty}$  this model is equivalent to the original one at  $\lim_{h \to 0} \lim_{L \to \infty}$  in the sense that the magnetization is parallel to certain axis labeled by i = 1. Some degeneracy still is present in (3), since two opposite ordering directions are equivalent, but this peculiarity does not play any role if we consider, e. g., the Greens function  $\widetilde{G}_i(\mathbf{x}) = \langle \varphi_i(\mathbf{0}) \varphi_i(\mathbf{x}) \rangle$ . In the Fourier representation, the correlation function  $G_i(\mathbf{k})$  is defined by

$$\langle \varphi_i(\mathbf{k}) \, \varphi_j(-\mathbf{k}) \rangle = \delta_{ij} \, G_i(\mathbf{k}) \,.$$
 (4)

Hamiltonian (3) is more suitable for our analysis than (1), since the equations derived in [5] can be easily generalized to include the symmetry breaking term  $\delta \cdot \varphi_1^2(\mathbf{x})$ . It is incorporated in the Gaussian part of the Hamiltonian

$$H_0/T = \sum_{i,\mathbf{k}} \left( r_0 - \delta \cdot \delta_{i,1} + c\mathbf{k}^2 \right) |\varphi_i(\mathbf{k})|^2 .$$
 (5)

As a result, the Dyson equation in [5] becomes

$$\frac{1}{2G_i(\mathbf{k})} = r_0 - \delta \cdot \delta_{i,1} + ck^2 - \frac{\partial D(G)}{\partial G_i(\mathbf{k})} + \vartheta_i(\mathbf{k})$$
 (6)

where D(G) is a quantity, the diagram expansion of which contains all skeleton diagrams (i. e., those connected diagrams without outer lines containing no parts like  $\longrightarrow$  ), constructed of the fourth order vertices  $\longrightarrow$  . The solid coupling lines in the diagrams are related to the correlation function  $G_i(\mathbf{k})$ , but the dashed lines to  $-V^{-1}u_{\mathbf{k}} = -V^{-1}\int u(\mathbf{x})e^{-i\mathbf{k}\mathbf{x}}d\mathbf{x}$ . Here the notation  $u_{\mathbf{k}} = u\,\tilde{u}_{\mathbf{k}}$  is used for a generalization, while the actual case of interest is  $\tilde{u}_{\mathbf{k}} \equiv 1$ . Any two solid lines connected to the same kink (node) have the same index i. According to the definition, Eq. (6) is exact. It is ensured including the remainder term  $\vartheta_i(\mathbf{k})$  which does not contribute to the perturbation expansion in u power series. Quantity D(G) is given by

$$D(G) = D^*(G, 1) + \bigcirc -- \bigcirc$$
 (7)

where  $D^*(G,\zeta)$  is the solution of the differential equation

$$D^*(G,\zeta) = -\frac{1}{2} \sum_{\mathbf{q}} \ln[1 - 2\Sigma(\mathbf{q},\zeta)] - \zeta \frac{\partial}{\partial \zeta} D^*(G,\zeta)$$
 (8)

with the boundary condition

$$D^*(G,0) = -\frac{1}{2} \sum_{\mathbf{q}} \ln[1 - 2\Sigma^{(0)}(\mathbf{q})], \qquad (9)$$

where

$$\Sigma^{(0)}(\mathbf{q}) = -2u_{\mathbf{q}}V^{-1}\sum_{i,\mathbf{k}}G_i(\mathbf{k})G_i(\mathbf{q} - \mathbf{k}).$$
(10)

Here  $\Sigma(\mathbf{q},\zeta)$  is a quantity having the diagram expansion

$$\Sigma(\mathbf{q},\zeta) = \frac{\mathbf{q}}{\mathbf{q}} + \zeta \frac{\mathbf{q}}{\mathbf{q}} + \zeta^{2} \left\{ \frac{\mathbf{q}}{\mathbf{q}} + \zeta^{2} \left\{ \frac{\mathbf{q}}{\mathbf{q}} \right\} \right\} + \dots$$

$$(11)$$

$$\overset{\mathbf{k}}{\sim} \sim \overset{\mathbf{k}}{\sim} = -u_{\mathbf{k}} V^{-1} / \left[ 1 - 2\Sigma(\mathbf{k}, \zeta) \right]$$
 (12)

corresponding to the waved lines, and factor  $-V^{-1}u_{\mathbf{q}}$  corresponding to a pair of fixed (formally considered as nonequivalent) broken dashed lines in (11). Quantity  $\Sigma(\mathbf{q},\zeta)$  is defined by converging sum and integrals (cf. Sec. 4.7 and Appendix A in [5]), i. e.,

$$\Sigma(\mathbf{q},\zeta) = \Sigma^{(0)}(\mathbf{q}) + \int_{0}^{u^{-p}} e^{-t_1} dt_1 \int_{0}^{u^{-p}} e^{-t_2} B(\mathbf{q},\zeta,t_1t_2) dt_2 , \qquad (13)$$

$$B(\mathbf{q},\zeta,t) = \sum_{n=1}^{\infty} \frac{\zeta^n t^n}{(n!)^2} \Sigma^{(n)}(\mathbf{q},\zeta) , \qquad (14)$$

where  $\Sigma^{(n)}(\mathbf{q},\zeta)$  represents the sum of diagrams of the *n*-th order in (11), and *p* is a constant 0 . Note that the zeroth-order term is given by Eq. (10).

Based on these equations of the GFD theory, we have derived the possible values of the exact critical exponents  $\gamma$  and  $\nu$  describing the divergence of susceptibility, i. e.  $\chi \propto (T - T_c)^{-\gamma}$ , and correlation length, i. e.  $\xi \propto (T - T_c)^{-\nu}$ , when approaching the critical point  $T = T_c$  from higher temperatures. These values at the spatial dimensionality d = 2, 3 and the dimensionality of the order parameter  $n = 1, 2, 3, \ldots$  (only the case n = 1 is meaningful at d = 2) are [5]

$$\gamma = \frac{d+2j+4m}{d(1+m+j)-2j}$$
 (15)

$$\nu = \frac{2(1+m)+j}{d(1+m+j)-2j} \tag{16}$$

where m may have values  $m = 1, 2, 3, \ldots$ , and j may have values  $j = -m, -m + 1, -m + 2, \ldots$  A general hypothesis relating the values of m and j to different models, as well as corrections to scaling for different physical quantities and several numerical tests have been discussed in [11, 12]. Here we only mention that m = 3 and j = 0 holds at n = 1 to coincide with the known exact results for 2D Ising model.

Since our equations contain the diagram expansion in terms of the true correlation function  $G_i(\mathbf{k})$  instead of the Gaussian one, they allow an analytic continuation from the region  $r_0 > 0$ , where they have an obvious physical solution [5], to arbitrary  $r_0$  value. One has to start with a finite volume, considering the thermodynamic limit afterwards. In this paper we have extended our analysis to include the region of negative  $r_0$  values below the critical point and to study the transverse and longitudinal fluctuations of the order parameter field in presence of an infinitesimal external field.

# 3 Alternative formulation of the basic equations

An alternative formulation of our diagrammatic equations can be helpful to prove some basic properties of the solution (see the end of Appendix). Namely, a resummation of the self-energy diagrams contained in  $R_i(\mathbf{k}) = -\partial D^*(G, 1)/\partial G_i(\mathbf{k})$  can be used instead of (8).

As discussed in [5], these are skeleton diagrams like  $\frac{\mathbf{k} \times \mathbf{k} \cdot \mathbf{k}}{\mathbf{k} \cdot \mathbf{k}}$  with two outer solid lines, obtained by breaking one solid line with wave vector  $\mathbf{k}$  in the coupled skeleton diagrams of  $D^*(G,1)$ . According to our notation, the factors of the lines marked by crosses are omitted, and "coupled" means that the diagram does not contain outer lines. The summation over the linear chains of blocks -- contained in the self–energy diagrams of  $R_i(\mathbf{k})$ 

can be performed, as it has been done in [5] with the diagrams of  $\Sigma(\mathbf{k},\zeta)$ . It yields the expansion of  $R_i(\mathbf{k})$  represented by skeleton diagrams where the true correlation function  $G_i(\mathbf{k})$  is related to the solid lines and the dashed lines are replaced by the waved lines. Like in (11), these diagrams do not contain parts — and  $\sim$  and  $\sim$  . According to (7), the diagram  $\rightarrow$ — is not included in  $D^*(G,1)$ , and it also cannot be involved in the actual grouping of diagrams since the extension of dashed line by adding the blocks ———— would yield non–skeleton diagrams in this case. In such a way, we have the expansion

$$-R_{i}(\mathbf{k}) = \underline{\mathbf{i}}, \underline{\mathbf{k}} \times \underbrace{\mathbf{k}}_{\mathbf{X}} + \underline{\mathbf{i}}, \underline{\mathbf{k}} + \underline{\mathbf{i}}, \underline{\mathbf{k}} \times \underline{\mathbf{k}} + \dots$$
 (17)

Here we have indicated explicitly that certain index  $1 \le i \le n$  refers to the outer lines in the n-component case. The waved line, given by (12), corresponds to  $\zeta = 1$ . The combinatorial factors 4, 32, etc., are included in the diagrams not distinguishing the two orientations with respect to the vectors  $\mathbf{k}$  and  $-\mathbf{k}$  as different. The resummation of expansion (17) can be made by adopting our method presented by Eqs. (13) and (14).

The Dyson equation (6) can be formulated in accordance with the variational principle, i. e., it follows from the extremum condition  $\partial \tilde{F}(G)/\partial G_i(\mathbf{k}) = 0$  of the reduced free energy function

$$\widetilde{F}(G) = -\frac{1}{2} \sum_{i,\mathbf{k}} \ln\left[2\pi G_i(\mathbf{k})\right] + \sum_{i,\mathbf{k}} \left[\theta_i(\mathbf{k}) G_i(\mathbf{k}) - \frac{1}{2}\right] - D(G) . \tag{18}$$

Here  $\theta_i(\mathbf{k}) = r_0 - \delta \cdot \delta_{i,1} + ck^2$  and  $\widetilde{F}(G)$  depends on the set of discrete variables  $G_i(\mathbf{k})$ , as consistent with the diagrammatic definition of D(G). This function is related to the free energy  $F = -T \ln Z$  via  $\widetilde{F}(G) = F/T$ . First it has been obtained in [26] for the case n = 1. The fact that  $\widetilde{F}(G)$  provides the diagrammatic representation of the reduced free energy can be proven as follows. According to (6),  $\partial \widetilde{F}(G)/\partial G_i(\mathbf{k}) = 0$  holds, neglecting the remainder term  $\vartheta_i(\mathbf{k})$ . It means that

$$\frac{\partial \widetilde{F}}{\partial r_0} = \sum_{i,\mathbf{k}} G_i(\mathbf{k}) = V \langle \varphi^2(\mathbf{x}) \rangle \equiv \frac{\partial (F/T)}{\partial r_0}$$
(19)

is true within the diagrammatic perturbation theory. Besides, it is straightforward to check that  $\tilde{F}(G) = F/T$  holds at  $r_0 \to +\infty$ . By integration in (19) over  $r_0$  from  $+\infty$  to any finite value we find that  $\tilde{F}(G) = F/T$  is valid in general.

# 4 The correlation function and susceptibility below $T_c$

Some important relations between the correlation function, the long–range order parameter M (e. g., magnetization or polarization), and susceptibility  $\chi$ , following directly from the first principles, are considered in this section.

We have defined the correlation function in the coordinate representation as

$$\widetilde{G}_i(\mathbf{x}) = \langle \varphi_i(\mathbf{x}_1) \, \varphi_i(\mathbf{x}_1 + \mathbf{x}) \rangle = V^{-1} \sum_{\mathbf{k}} G_i(\mathbf{k}) \, e^{i\mathbf{k}\mathbf{x}} \,.$$
 (20)

For simplicity, first, let us consider the one–component case. In this case (omitting the index i) we have [7]

$$M^2 = \lim_{x \to \infty} \tilde{G}(\mathbf{x}) = G(\mathbf{0})/V$$
 at  $V \to \infty$ , (21)

or

$$\widetilde{G}(\mathbf{x}) = M^2 + \widetilde{G}'(\mathbf{x}) , \qquad (22)$$

where  $\widetilde{G}'(\mathbf{x})$  tends to zero if  $x \to \infty$ . In the Fourier representation (22) reduces to

$$G(\mathbf{k}) = \delta_{\mathbf{k},\mathbf{0}} V M^2 + G'(\mathbf{k})$$
(23)

where  $G'(\mathbf{k})$  is the Fourier transform of  $\widetilde{G}'(\mathbf{x})$ . The susceptibility, calculated directly from the Gibbs distribution, is

$$\chi = \lim_{h \to 0} \lim_{L \to \infty} \frac{\partial \langle \varphi \rangle}{\partial h} = \lim_{h \to 0} \lim_{L \to \infty} \int \left( \widetilde{G}(\mathbf{x}) - \langle \varphi \rangle^2 \right) d\mathbf{x} = G'(\mathbf{0}) . \tag{24}$$

In this limit  $\langle \varphi \rangle = M$  holds, the latter, however, is not correct at h = 0 when  $\langle \varphi \rangle = 0$ . The considered limit for  $\chi$  exists and  $G'(\mathbf{0})$  has a finite value in our case of n = 1, since the correlation function  $\tilde{G}'(\mathbf{x})$  is characterized by a finite correlation length  $\xi$ , which ensures the convergence of the integral in (24).

Consider now the case n > 1. If an external field is applied along the i-th axis with i = 1 (even if  $h \to 0$ ), the longitudinal Greens function  $G_{\parallel}(\mathbf{k}) \equiv G_1(\mathbf{k})$  behaves in a different way than the transverse one  $G_{\perp}(\mathbf{k}) \equiv G_j(\mathbf{k})$  with  $j \neq 1$ . It is a rigorously stated fact [3] that  $G_{\perp}(\mathbf{0})$  diverges as M/h if  $h \to 0$  below  $T_c$ , which is related to the divergence of the transverse susceptibility in this case. In analogy to (23) and (24) we have

$$G_{\parallel}(\mathbf{k}) = \delta_{\mathbf{k},\mathbf{0}} V M^2 + G'_{\parallel}(\mathbf{k}) ,$$
 (25)

$$\chi_{\parallel}(h) = \partial M/\partial h = G'_{\parallel}(\mathbf{0}) .$$
 (26)

Our further analysis shows that the longitudinal susceptibility  $\chi_{\parallel}(h)$  diverges at  $h \to 0$  for 2 < d < 4 and n > 1, i. e.,  $G'_{\parallel}(\mathbf{k})$  diverges at  $k \to 0$ . Note that  $G'_{\parallel}(\mathbf{k}) = G_{\parallel}(\mathbf{k})$  holds at  $\mathbf{k} \neq \mathbf{0}$ . The long-wavelength divergences of the transverse and longitudinal correlation functions below  $T_c$  is known in literature as the Goldstone mode singularities established by the Goldstone theorem [27, 15].

# 5 Generalized scaling hypothesis

According to the known [3] scaling hypothesis, the correlation function above the critical point, i. e. at  $T > T_c$  and  $T \to T_c$ , can be represented in a scaled form

$$G_i(\mathbf{k}) \simeq \xi^{2-\eta} g_i(k\xi) ,$$
 (27)

where  $\xi$  is the correlation length,  $\eta$  is the critical exponent, and  $g_i(z)$  is a scaling function. Since  $\xi \sim t^{-\nu}$  holds, where  $t = (T/T_c) - 1$  is the reduced temperature, the correlation function can be represented also as

$$G_i(\mathbf{k}) \simeq t^{-\gamma} g_i \left( k t^{-\nu} \right) ,$$
 (28)

where  $\gamma = (2 - \eta)\nu$ . Since the phase transition occurs merely at a single point h = t = 0 in the h-t plane, there exists a way how the scaling relations like (27) or (28) can be continued to the region t < 0 passing the singular point h = t = 0. Eq. (27) is not valid at h = 0 and t < 0 in the case of n > 1, since  $G'_{\parallel}(\mathbf{0})$  and, therefore, the correlation length

 $\xi$  diverges at  $h \to 0$  [cf. Eq. (24)]. The known scaling relations are recovered assuming that the physical picture remains similar if we approach the critical point like  $t \to s t$  and  $h \to s^{\sigma} h$ , where s < 1 is the rescaling factor. Thus, the distance from the critical point  $\hat{t} = (t^2 + h^{2/\sigma})^{1/2}$  and the polar angle  $\theta = \arctan(h^{1/\sigma}/t)$  in the  $t - h^{1/\sigma}$  plane are two relevant scaling arguments. According to this discussion, a suitable generalization of the scaling relation (28) is

$$G_i(\mathbf{k}) \simeq \hat{t}^{-\gamma} g_i \left( k \hat{t}^{-\nu}, \theta \right) ,$$
 (29)

which is true at  $\hat{t} \to 0$  for any given values of  $k\hat{t}^{-\nu}$  and  $\theta$ . Consider  $G_{\perp}(\mathbf{0})$  at a small negative t. Taking into account that  $h^{1/\sigma} \simeq \hat{t} (\pi - \theta)$  and  $M \propto (-t)^{\beta} \simeq h^{\beta/\sigma} (\pi - \theta)^{-\beta}$  hold at  $\theta \to \pi$ , the correct result  $G_{\perp}(\mathbf{0}) \simeq M/h$  is obtained in this limit if  $g_{\perp}(0,\theta) \propto (\pi - \theta)^{-\sigma}$ holds at  $\pi - \theta \to 0$  and the scaling dimension is  $\sigma = \beta + \gamma$ . By generalizing the scaling relation  $M \propto (-t)^{\beta}$  to  $M \propto \hat{t}^{\beta}$  (at a fixed  $\theta$ ) we obtain also the correct behavior  $M \propto h^{1/\delta}$ at t=0, where  $\delta=1+\gamma/\beta$ . Eq. (29) makes sense for  $G_{\parallel}(\mathbf{k})$  at  $\mathbf{k}\neq\mathbf{0}$ . According to (25) and (26), the longitudinal susceptibility is  $\chi_{\parallel} = G'_{\parallel}(\mathbf{0}) = G_{\parallel}(+0)$ , where  $G_{\parallel}(+0)$  denotes the value of the Greens function at an infinitely small, but nonzero k value. It is easy to check that (29) reproduces the known scaling behavior of  $\chi_{\parallel}$  for  $t \geq 0$  both at h = 0 $(\chi_{\parallel} \propto t^{-\gamma})$  and at t = 0  $(\chi_{\parallel} \propto h^{\frac{1}{\delta}-1})$ . In the limit  $h \to 0$  Eq. (29) yields

$$G_{i}(\mathbf{k}) \simeq |t|^{-\gamma} g_{i}^{+} (k |t|^{-\nu}) \quad \text{at} \quad t > 0$$

$$G_{i}(\mathbf{k}) \simeq |t|^{-\gamma} g_{i}^{-} (k |t|^{-\nu}) \quad \text{at} \quad t < 0 ,$$

$$(30)$$

$$G_i(\mathbf{k}) \simeq |t|^{-\gamma} g_i^-(k|t|^{-\nu}) \quad \text{at} \quad t < 0,$$
 (31)

where  $g_i^+(z) = g_i(z,0)$  and  $g_i^-(z) = g_i(z,\pi)$ . The analysis of our diagrammatic equations confirm the scaling relations (30) and (31). It shows also that, in the case of the order parameter dimensionality n > 1, both the longitudinal and the transverse Greens functions diverge at  $k \to 0$  when  $T < T_c$ . It means that  $g_i^-(z)$  diverges at  $z \to 0$  for n > 1. In any case we have  $g_i^{\pm}(z) \propto z^{-2+\eta}$  at  $z \to \infty$ , which means that the correlation function continuously transforms to the known critical Greens function  $G_i(\mathbf{k}) \sim k^{-2+\eta}$  at  $t \to 0$ .

#### 6 Exact scaling relations and their consequences

In distinction to Sec. 5, here we consider other kind of scaling relations which also are relevant to our further analysis. These are exact and rigorous relations between the correlation function and parameters of the Hamiltonian  $H/T = H_0/T + H_1/T$ , where  $H_0/T$ is given by (5) and  $H_1/T$  represents the  $\varphi^4$  contribution (2) at  $u_{\mathbf{k}} = u$ .

Following the method described in Appendix B of [5], the Hamiltonian H/T is transformed to

$$H/T = \sum_{i,\mathbf{p}} \left( R - \epsilon \cdot \delta_{i,1} + \mathbf{p}^2 \right) | \Psi_i(\mathbf{p}) |^2$$

$$+ V_1^{-1} \sum_{i,j,\mathbf{p}_1,\mathbf{p}_2,\mathbf{p}_3} \Psi_i(\mathbf{p}_1) \Psi_i(\mathbf{p}_2) \Psi_j(\mathbf{p}_3) \Psi_j(-\mathbf{p}_1 - \mathbf{p}_2 - \mathbf{p}_3) ,$$

$$(32)$$

where  $\Psi_i(\mathbf{p}) = u^{\alpha} c^{-d\alpha/2} \varphi_i(\mathbf{k}), \ \mathbf{p} = c^{2\alpha} u^{-\alpha} \mathbf{k}, \ R = r_0 c^{d\alpha} u^{-2\alpha}, \ \text{and} \ \epsilon = \delta u^{-2\alpha} c^{d\alpha}.$  Here  $\alpha = 1/(4-d)$  and the summation over **p** takes place within  $p < p_0 = c^{2\alpha}u^{-\alpha}\Lambda$  in accordance with the rescaled volume  $V_1 = V c^{-2d\alpha} u^{d\alpha}$ . According to (32) we have

$$G_i(\mathbf{k}) = \left\langle |\varphi_i(\mathbf{k})|^2 \right\rangle = c^{d\alpha} u^{-2\alpha} \left\langle |\Psi_i(\mathbf{p})|^2 \right\rangle = c^{d\alpha} u^{-2\alpha} \widetilde{g}_i(\mathbf{p}, p_0, R, \epsilon, V_1) , \qquad (33)$$

where, at fixed d and n,  $\tilde{g}_i$  is a function of the given arguments only. The thermodynamic limit exists at  $\mathbf{k} \neq \mathbf{0}$ , so that in this case we can write

$$\lim_{\delta \to 0} \lim_{V \to \infty} G_i(\mathbf{k}) = c^{d\alpha} u^{-2\alpha} \hat{g}_i(\mathbf{p}, p_0, R) , \qquad (34)$$

where the scaling function  $\hat{g}_i$  represents the limit of  $\tilde{g}_i$ . If R is varied, then the model with Hamiltonian (32) undergoes the second-order phase transition at some critical value  $R = R_c(p_0) < 0$ . Thus, Eq. (34) can be rewritten in new variables with a scaling function  $g_i(\mathbf{p}, p_0, t)$ , where  $t = 1 - (R/R_c) = 1 - (r_0/r_{0c})$  is the reduced temperature,  $r_{0c}$  being the critical value of  $r_0$ . Thus, we have

$$\hat{g}_i(\mathbf{p}, p_0, R) = g_i(\mathbf{p}, p_0, t) . \tag{35}$$

Based on (34) and (35), we can make some conclusions about the scaling of the critical region for the reduced temperature t, as well as for the wave vector  $\mathbf{k}$  at t=0 and also at a fixed t<0. The latter case is relevant for the long-wave limit  $k\to 0$  at n>1. By the critical region we mean the region inside of which the correlation function is well described by a certain asymptotical law. According to (34) and (35), the width of the critical region  $t_{crit}$  or  $k_{crit}$ , as well as the coefficients in asymptotic expansions in powers of k at a fixed t (t=0 for  $n \ge 1$  or t<0 for n>1) can be written in a scaled form with (or without) power-like prefactors and scaling functions containing single argument  $p_0 = c^{2\alpha}u^{-\alpha}\Lambda$ .

The limit  $u \to 0$  is important in our consideration. To extract exact critical exponents from our equations, it has to be ensured that, inside the critical region, the remainder term  $\vartheta_i(\mathbf{k})$  in (6) is much smaller than any term in the asymptotic expansion of  $1/G_i(\mathbf{k})$ . This is possible at  $u \to 0$  if these expansion terms and also the width of the critical region do not tend to zero faster than any positive power of u [5]. For the scaling functions of  $p_0$ , the limit  $u \to 0$  is equivalent to the limit  $\Lambda \to \infty$  at d < 4. The relevant quantities  $(t_{crit},$  $k_{crit}$ , and expansion coefficients at k powers) can tend to zero exponentially at  $u \to 0$  only if the corresponding scaling functions of  $c^{2\alpha}u^{-\alpha}\Lambda$  do so. The latter would mean that these quantities are very strongly (exponentially) affected by any relatively small variation of the upper cutoff parameter  $\Lambda$  at large  $\Lambda$  values. It seems to be rather unphysical, since the long-wave behavior at a fixed t (also at t < 0) cannot be so sensitive to small variations in the short-range interactions. Due to the joining of the asymptotic solutions, the fact that the expansion coefficients in k power series at t=0 are not exponentially small in u means also that the same is true for the expansion coefficients in |t| power series at  $|t| \to 0$ . Thus, only the remainder term  $\vartheta_i(\mathbf{k})$  tends to zero faster than  $u^s$  at any s>0, provided that our solution represents an analytic continuation (see the end of Sec. 2) from the stable domain  $r_0 > 0$  where our equations have originated and where this basic property of  $\vartheta_i(\mathbf{k})$ follows directly from our derivations. It implies, in particular, that the solution below  $T_c$  should coincide with (31), as consistent with the existence of continuous second-order phase transition. If we have a smooth solution of this kind, then the critical exponents can be determined by considering suitable limits [5]  $(u \to 0 \text{ and } k \sim u^r k_{crit}(u), \text{ or } u \to 0$ and  $t \sim u^{r/\nu} t_{crit}(u)$  with r > 0) not only at  $T = T_c$  and  $T \to T_c$ , but also at  $T < T_c$ . In this case the remainder term  $\vartheta_i(\mathbf{k})$  is negligibly small [5].

### 7 The low–temperature solution at n = 1

Let us now consider the solution of our equations below the critical point starting with the case n = 1. The symmetry breaking term with  $\delta$  is irrelevant at n = 1, therefore we set  $\delta = 0$ . According to (21),  $1/G(\mathbf{k})$  vanishes at  $\mathbf{k} = \mathbf{0}$  in the thermodynamic limit  $V \to \infty$ , so that the equation (6) (taking into account (7) and omitting the irrelevant correction  $\vartheta_i(\mathbf{k})$ ) for scalar order–parameter field (n = 1) can be written as

$$1/(2G_1(\mathbf{k})) = ck^2 + R_1(\mathbf{k}) - R_1(\mathbf{0}) \quad \text{at } \mathbf{k} \neq \mathbf{0} ,$$
 (36)

$$1/(2G_1(\mathbf{0})) = r_0 + 2u\tilde{G} + R_1(\mathbf{0}) = 0,$$
(37)

where (for arbitrary n)

$$\widetilde{G} = \left\langle \varphi^2(\mathbf{x}) \right\rangle = V^{-1} \sum_{i,\mathbf{k}} G_i(\mathbf{k}) ,$$
(38)

$$R_i(\mathbf{k}) = -\frac{\partial D^*(G, 1)}{\partial G_i(\mathbf{k})} . \tag{39}$$

To simplify the notation, further we shall omit the index  $i \equiv 1$  in the actual case of n = 1. According to (21), single term with  $\mathbf{k} = \mathbf{0}$  gives a nonvanishing contribution to (38) at  $V \to \infty$ , while the contribution of all other terms may be replaced by an integral, i. e.,

$$\widetilde{G} = M^2 + (2\pi)^{-d} \int G'(\mathbf{k}) d\mathbf{k} . \tag{40}$$

Similarly, terms with  $M^2$ ,  $M^4$ ,  $M^6$ , etc. appear in (11) due to the contributions provided by zero–vectors related to some of the solid lines. For instance, the zeroth–order term (10) reads

$$\Sigma^{(0)}(\mathbf{q}) = -2u \left( 2M^2 G(\mathbf{q}) + (2\pi)^{-d} \int G'(\mathbf{k}) G'(\mathbf{q} - \mathbf{k}) d\mathbf{k} \right) . \tag{41}$$

The terms with the spontaneous magnetization M appear in our equations in a natural way if we first consider a very large, but finite volume V, which then is tended to infinity. They appear as a feedback which does not allow the right hand side of (37) to become negative, by keeping it at  $1/(2G(\mathbf{0})) \sim 1/V$ , when  $r_0$  goes to large enough negative values.

The actual model at n=1 belongs to the Ising universality class characterized by a finite correlation length at  $T < T_c$ . It means that  $G'(\mathbf{0})$  has a finite value and  $1/G(\mathbf{k})$  transforms to zero at  $\mathbf{k} = \mathbf{0}$  by a jump. According to (36), it means that  $R(+0) \neq R(\mathbf{0})$  holds, where the value of  $R(\mathbf{k})$  at an infinitesimal non–zero k is denoted by R(+0). To show that this is really possible, consider the contribution (denoted by  $R^{(0)}(\mathbf{k})$ ) of the first diagram in (11) which yields

$$R^{(0)}(+0) = R^{(0)}(\mathbf{0}) + \frac{4u M^2}{1 + 4u \left(2M^2 G'(\mathbf{0}) + (2\pi)^{-d} \int G'^2(\mathbf{q}) d\mathbf{q}\right)}.$$
 (42)

From (42) we see that  $R(+0) \neq R(\mathbf{0})$  holds, in general, if  $G'(\mathbf{0})$  has a finite value. Therefore such a selfconsistent solution is, in principle, possible.

Consider now the solution at  $r_0 \to -\infty$  and small u, i. e., at low temperatures. In this case we find a solution such that

$$M^2 = -r_0/(2u)$$
,  $G(\mathbf{k}) = -1/(Ar_0)$ ,  $\Sigma(\mathbf{k}, \zeta) = f(\zeta, A)$ , (43)

hold at any fixed u > 0 and  $\mathbf{k} \neq \mathbf{0}$ , if  $r_0 \to -\infty$ , where A is a constant independent of  $r_0$ , c, and  $\Lambda$ ,  $f(\zeta, A)$  is a function of the given arguments. One expects that A tends to some universal constant at  $u \to 0$ . In this case, at A = 4, our solution coincides with the Gaussian approximation

$$G'(\mathbf{k}) = \frac{1}{-4r_0 + 2ck^2} \,. \tag{44}$$

The correction  $\sim ck^2$  has been neglected in (43).

Condition  $M^2 = -r_0/(2u)$ , corresponding to the minimum of (3), holds for any physical solution if  $r_0 \to -\infty$  since fluctuations are suppressed. This follows from (37) and (40), if the main terms  $r_0$  and  $2u M^2$  are retained in (37).

Quantity  $\Sigma(\mathbf{0}, \zeta)$  in the denominator of (12) diverges in the thermodynamic limit  $V \to \infty$  like V or even faster, i. e., like  $V^{\mu}$  with  $\mu \geq 1$ , as shown in Appendix. The divergence appears due to the special contributions provided by zero wave vectors  $\mathbf{k} = \mathbf{0}$  related to some of the solid lines in the diagram expansion (11) of  $\Sigma(\mathbf{0}, \zeta)$  at  $T < T_c$ . These diverging terms make the analysis below  $T_c$  more difficult as compared to the case  $T \geq T_c$  discussed in [5].

In spite of the divergence of  $\Sigma(\mathbf{0},\zeta)$ , a single term with  $\mathbf{q}=\mathbf{0}$  in (8) does not contribute to  $D^*(G,\zeta)$  and  $R(\mathbf{k})$  if  $V\to\infty$ . Really, if  $\Sigma(\mathbf{0},\zeta)$  diverges as  $-(V/V_0)^s$  ( $V_0$  is the volume of an elementary cell) with s>0, then this single term is approximately  $-(s/2)\cdot\ln(V/V_0)$ , whereas the whole sum is proportional to  $V/V_0$ . On the other hand,  $\Sigma(\mathbf{0},\zeta)$  appears in the denominator of the corresponding term if the derivative with respect to  $G(\mathbf{k})$  is calculated in (8), therefore, this term cannot be by a factor V larger than other terms, i. e., it cannot give an especial contribution.

The perturbation sum for  $\Sigma(\mathbf{k},\zeta)$  at  $\mathbf{k}\neq\mathbf{0}$  also contains terms diverging at  $V\to\infty$ . In a normal case, the constraint  $\mathbf{k}=\mathbf{0}$  for wave vectors of m solid lines in a diagram means removal of m integrations over wave vectors. However, for some distributions of the zero-vectors this condition is violated, which yields the diverging terms. We have shown in

Appendix that the divergent terms contain insertions like, e. g., 0 0 with 2m outer solid lines having fixed  $\mathbf{k} = \mathbf{0}$  vectors. As shown in Appendix, a resummation of these insertions gives a non-divergent result. Besides, the simplified analysis which ignores these insertions is qualitatively correct, as regards the general scaling form of the solution. However, for a complete formal correctness we should take into account the fact that specific values of scaling functions can be renormalized by these zero-vector-cumulant (see Appendix for explanation) insertions. Further we shall call the terms without such insertions the "normal" terms or contributions. Our results at  $T < T_c$  are completely consistent with those at  $T = T_c$  and  $T > T_c$  and agree with the non-perturbative RG analysis provided in Sec. 9.5. It confirms the statements made in this paragraph.

An important property of the "normal" contributions to  $\Sigma(\mathbf{k},\zeta)$  at  $\mathbf{k} \neq \mathbf{0}$  is that any term, where zero wave vector is related to a waved line, vanishes in the thermodynamic limit  $V \to \infty$ . It holds because the waved line vanishes due to the divergence of  $\Sigma(\mathbf{0},\zeta)$ .

Condition  $\Sigma(\mathbf{k},\zeta) = f(\zeta,A)$  at  $\mathbf{k} \neq \mathbf{0}$  holds if  $r_0 \to -\infty$  because  $\Sigma^{(0)}(\mathbf{q})$  and all terms of the sum (14) in this limit depend merely on parameters  $\zeta$  and A for any fixed u. The latter is true in the approximation where no zero-vector-cumulants are included, since the main terms come from the diagrams in (11) if we extract the contribution, containing no integrals, where one half of the solid lines have zero wave vectors  $\mathbf{k} = \mathbf{0}$  (it yields a factor  $M^2$  for the first diagram,  $M^4$  – for the second diagram, and so on). Besides, the

waved lines should have nonzero wave vectors, as explained before. According to (43) each replacement of  $G(\mathbf{0})/V = M^2$  by an integral over wave vectors produces a factor  $\sim r_0^{-2}$ . This is the reason why the main terms at  $r_0 \to -\infty$  contain no integrals.

These main terms lead to asymptotic solutions (at  $r_0 \to -\infty$ ) for quantities  $\partial \Sigma(\mathbf{q}, \zeta)/\partial G(\mathbf{k})$  and  $\partial D^*(G, \zeta)/\partial G(\mathbf{k})$  at  $\mathbf{q} = \mathbf{k} \neq \mathbf{0}$  in the form where  $r_0$  is multiplied by some function of  $\zeta$  and A, namely,  $R(\mathbf{k}) = -Q(A) r_0$ . This main contribution vanishes at  $\mathbf{k} = \mathbf{0}$ , since the derivation  $\partial \Sigma(\mathbf{0}, \zeta)/\partial G(\mathbf{0})$ , implicated in the calculation of  $R(\mathbf{0})$ , means removal of a diverging factor  $G(\mathbf{0}) \sim V$ . Quantity  $\Sigma(\mathbf{0}, \zeta)$  diverges, whereas the waved lines in this case contain vanishing factors  $\sim 1/\Sigma(\mathbf{0}, \zeta)$  providing finite value of the derivative at  $V \to \infty$ . Therefore, by substituting  $R(\mathbf{k}) = -Q(A) r_0$  into (36) and retaining only the leading terms, we obtain a selfconsistent equation 2Q(A) = A for the unknown amplitude A. Following the consideration in Appendix, the inclusion of zero-vector-cumulant insertions can merely renormalize the function Q(A).

# 8 Asymptotic solution at $T \to T_c$

Our equations provide the asymptotic solution at  $T \to T_c$ , where  $T < T_c$ , in the scaled form (31) which allows a unified description provided here for  $n \ge 1$ .

Like in [5], here we assume that  $r_0$  is the only parameter in (3) which depends on temperature T and the dependence is linear. At the critical point  $r_0 = r_{0c}$  we have  $1/G_i(+0) = 0$  for all i at  $\lim_{\delta \to 0} \lim_{V \to \infty}$ , so that the Dyson equation (6) in this limit reads

$$\frac{1}{2G_i(+0)} = -\frac{dr_0}{dT} \cdot \Delta + 2u \left( \tilde{G} - \tilde{G}^* \right) + R_i(+0) - R_i^*(+0)$$
 (45)

$$\frac{1}{2G_i(\mathbf{k})} - \frac{1}{2G_i(+0)} = ck^2 + R_i(\mathbf{k}) - R_i(+0) . \tag{46}$$

Here  $\Delta = |T - T_c|$  is an analog of |t| in (31),  $\tilde{G}^*$  and  $R_i^*(+0) \equiv R_i^*(\mathbf{0})$  are the values of  $\tilde{G}$  and  $R_i(\mathbf{0})$  calculated at the critical Greens function  $G_i(\mathbf{k}) = G_i^*(\mathbf{k})$  considered as a known fixed quantity. Due to the symmetry breaking term  $\delta \cdot \delta_{i,1}$  in (3), only the longitudinal component  $1/G_1(\mathbf{0}) \equiv 1/G_{\parallel}(\mathbf{0})$  becomes as small as  $\sim 1/V$  when  $r_0$  is decreased below  $r_{0c}$ , giving rise to the magnetization  $M^2 = G_{\parallel}(\mathbf{0})/V$ . According to (46), the condition  $1/G_{\parallel}(\mathbf{0}) = 0$  at  $V \to \infty$  means

$$1/\left(2G_{\parallel}(+0)\right) = R_{\parallel}(+0) - R_{\parallel}(\mathbf{0}) . \tag{47}$$

Equations (45) and (46) are analogous to (48) and (49) in [5] derived for  $T > T_c$ , and similar method of analysis is valid. Namely, correct results for the Greens function within the asymptotical region  $k \sim 1/\hat{\xi}$  can be obtained considering the limit  $u \to 0$  and  $\Delta \sim u^{r/\nu} \Delta_{crit}(u)$ , and formally cutting the integration over  $G_i(\mathbf{k})$  and  $G_i^*(\mathbf{k})$  in (45) and (46) by  $k < \Lambda = u^{-r} k_{crit}^{-1}(u)/\hat{\xi}$ . Here  $\Delta_{crit}(u)$  and  $k_{crit}(u)$  are the widths of the critical regions for  $\Delta$  and k, respectively, r is any positive constant, and  $\hat{\xi}$  is an analog of the correlation length. According to the generalized scaling hypothesis in Sec. 5, one may set  $\hat{\xi} = \xi(T = T + \Delta)$ . Note that our equations (45) to (47) do not contain  $r_{0c}$ . Only such a form is acceptable in this analysis: contrary to the critical exponents the critical temperature is essentially affected by the short–wave fluctuations.

We start our analysis with the "normal" (not diverging at  $V \to \infty$ ) terms discussed in Sec. 7 by using the well known scaling relation

$$2\beta = (d - 2 + \eta)\nu = d\nu - \gamma \tag{48}$$

relevant to  $M \sim \Delta^{\beta}$ . Our diagram equations become exact in the theoretical limits considered, and it allows in principle to find the exact critical exponents by solving these equations (Sec. 6). Therefore, the asymptotic solution satisfies the existing exact relations between the critical exponents, including (48). In fact, (48) is the necessary condition at which the diagrams below  $T_c$  have certain scaling properties, similar to those above  $T_c$ , where the exponents are common for the diagrams of all orders.

Selfconsistent solutions for  $\Sigma(\mathbf{q},\zeta)$  and for  $\partial D^*(G,\zeta)/\partial G_i(\mathbf{k})$  can be found at 2 < d < 4, having similar form as in the case  $T > T_c$  [5]. This is true for the "normal" terms because partial contributions in (13) proportional to  $M^0$ ,  $M^2$ ,  $M^4$ , etc., (corresponding to cases where zero-vectors are related to 0, 1, 2, etc., solid lines in diagrams (11)) have the same form and the same common factor  $\Delta^{-2\gamma+d\nu}$  as at  $T > T_c$ . It is easy to prove this property for diagrams of all orders by a simple normalization of all wave vectors to  $\Delta^{\nu}$ , like  $\mathbf{q}' = \mathbf{q}/\Delta^{\nu}$ , with the cutting of integration discussed above. Contrary to the case  $T > T_c$ , the main term of  $\partial \Sigma(\mathbf{q},\zeta)/\partial G_i(\mathbf{k})$  at  $T < T_c$  for given u, d, and n has the form

$$\partial \Sigma(\mathbf{q}, \zeta) / \partial G_i(\mathbf{k}) = V^{-1} \Delta^{-\gamma} Y_i(\mathbf{q}', \mathbf{k}', \zeta) + \delta_{i,1} \delta_{\mathbf{k}, \mathbf{q}} \Delta^{d\nu - \gamma} \hat{Y}(\mathbf{q}', \mathbf{k}', \zeta)$$
(49)

obtained by the above normalization, where  $\mathbf{k}' = \mathbf{k}\Delta^{-\nu}$ . The additional (second) term is due to the following. If in some diagrams of (11) the wave vectors for some solid lines are fixed  $\mathbf{k}_1 = \mathbf{0}$  (this yields an especial contribution merely at  $T < T_c$ ), then the wave vectors of some other solid lines also have a fixed value  $\mathbf{k}_2 = \mathbf{q}$ . This produces the second (extraordinary) term after derivation of the lines with a fixed wave vector  $\mathbf{q}$ . The simplest example is provided by the first diagram in (11) represented by (41). The first term in (41), which at arbitrary n reads  $-4u M^2 G_1(\mathbf{q})$ , yields an extraordinary contribution  $-4u \delta_{i,1} \delta_{\mathbf{q},\mathbf{k}} M^2$  to (49). In general, any diagram of (11) can be represented as two separate

The additional term in (49) essentially differs from the ordinary (first) term by factor  $\delta_{\mathbf{k},\mathbf{q}}V\Delta^{d\nu}$  because in this case the derivation procedure does not mean removal of integration over wave vectors. Both terms provide  $\partial D^*(G,\zeta)/\partial G_1(\mathbf{k}) = \Delta^{\gamma} \tilde{r}(\mathbf{k}',\zeta)$ , single term with  $\mathbf{q} = \mathbf{0}$  in (8) being negligible, as discussed in Sec.7. This scaled form is valid also for i > 1 and agree with that at  $T > T_c$  derived in [5]. The term with  $\delta_{\mathbf{k},\mathbf{q}}$  does not give a contribution to  $\partial D^*(G,\zeta)/\partial G_1(\mathbf{k})$  at  $V \to \infty$  if  $\mathbf{k} = \mathbf{0}$ : any of the partial contributions to  $\Sigma(\mathbf{0},\zeta)$ , where zero-vectors are related to the connecting solid lines in a configuration like

, is by a factor  $\sim G_1(\mathbf{0}) \equiv G_{\parallel}(\mathbf{0}) \simeq M^2 V$  larger than the corresponding term of  $\partial \Sigma(\mathbf{0}, \zeta)/\partial G_1(\mathbf{0})$ , where factor  $G_{\parallel}(\mathbf{0})$  is removed according to derivation of the connecting lines with  $\mathbf{k} = \mathbf{0}$ . No diverging factor is removed at k = +0 if  $G_{\parallel}(+0)$  has a finite value, therefore, R(+0) and  $R(\mathbf{0})$  are not identical at n = 1. In any case, this peculiarity refers only to the longitudinal component, so that  $R_{\perp}(+0) = R_{\perp}(\mathbf{0})$  holds in general.

The above discussed peculiarities with the extraordinary terms are irrelevant, as regards the exponents in the asymptotic expansion of  $G_i(\mathbf{k})$ . The magnetization M has corrections to scaling with the same exponents as other terms in (45) and (46) (although some expansion coefficients can be zero). This is consistent with the additional condition (47) – the equation for M. The corrections to scaling have the same origin at  $T < T_c$  and  $T > T_c$ : the term  $ck^2$  in (46) is by a factor  $\sim \Delta^{2\nu-\gamma}$  smaller than the leading term and the term "1" in (12) gives (in the same sense) a correction  $\sim \Delta^{2\gamma-d\nu}$ . In such a way, the general scaling form of the solution for  $R_i(\mathbf{k})$  and  $G_i(\mathbf{k})$  appears to be the same at  $T < T_c$  and  $T > T_c$ . Following the Appendix, it remains unchanged in the complete analysis which takes into account all possible distributions of  $\mathbf{k} = \mathbf{0}$  vectors in the diagrams of (11), and not only the "normal" contributions without the zero–vector–cumulant insertions.

Thus, for the spational dimensionality 2 < d < 4, the correlation function at  $T < T_c$  has similar singular structure as in the case of  $T > T_c$  [5], i. e., we have an asymptotic expansion

$$G_i(\mathbf{k}) = \sum_{\ell > 0} \Delta^{-\gamma + \gamma_\ell} g_i^{(\ell)} \left( \mathbf{k} \Delta^{-\nu} \right)$$
 (50)

with  $\gamma_0 = 0$  and correction exponents

$$\gamma_{\ell} = n_{\ell} \left( 2\nu - \gamma \right) + m_{\ell} \left( 2\gamma - d\nu \right) \tag{51}$$

valid for  $\ell \geq 1$ , where  $n_{\ell}$  and  $m_{\ell}$  are integer numbers  $\geq 0$ , and  $n_{\ell} + m_{\ell} \geq 1$ . Therefore, using the same arguments as in the case of  $T > T_c$  [5], we conclude that the possible values of exponents  $\gamma$  and  $\nu$  are given by (15) and (16). It agree with the generalized scaling hypothesis in Sec. 5 which tells us that the values of the exponents must be the same at  $T > T_c$  and  $T < T_c$ .

# 9 The asymptotic long-wave behavior below $T_c$ at n > 1

#### 9.1 Discussion of the existing results

According to the conventional believ [14, 17, 18, 19, 20, 21, 22, 23, 24, 25, 28], the transverse Greens function  $G_{\perp}(\mathbf{k})$  diverges like  $k^{-\lambda_{\perp}}$  with  $\lambda_{\perp} = 2$  at  $k \to 0$  below  $T_c$  for the systems with  $O(n \ge 2)$  rotational symmetry. It corresponds to the  $G_{\parallel}(\mathbf{k}) \sim k^{d-4}$  divergence of the longitudinal Greens function. Besides, the singular structure of the correlation functions is represented by an expansion in powers of  $k^{4-d}$  and  $k^{d-2}$  [22, 23]. Formally, our results agree with these ones at  $\lambda_{\perp} = 2$ . Nevertheless, below we will show that  $\lambda_{\perp} < 2$  holds near two dimensions at n = 2.

As usually accepted in lattice models, here (in this subsection) we define that all the parameters of the normalized Hamiltonian H/T (3) are proportional to the inverse temperature 1/T. In this case  $r_0$  is negative. We propose the following argument. The assumption that  $G_{\perp}(\mathbf{k}) \simeq a(T) k^{-2}$  holds (with some temperature–dependent amplitude

a(T)) in the stable region below the critical point, i. e., at  $T \leq T_c/C$ , where C is an arbitrarily large constant, leads to a conclusion that the critical temperature  $T_c$  continuously tends to zero at  $d \to 2$  (supposed d > 2). Really, at  $\lambda_{\perp} = 2$  we have

$$\left\langle \varphi^{2}(\mathbf{x}) \right\rangle = \frac{1}{V} \sum_{i,\mathbf{k}} G_{i}(\mathbf{k}) \simeq M^{2}$$

$$+ (2\pi)^{-d} \left[ \int G'_{\parallel}(\mathbf{k}) d\mathbf{k} + \frac{(n-1) S(d) \Lambda^{d-2} a(T)}{d-2} \right] ,$$
(52)

where S(d) is the area of unit sphere in d dimensions. Since the amplitude of the transverse fluctuations never can vanish at a finite temperature, Eq. (52) implies that the average  $\langle \varphi^2(\mathbf{x}) \rangle$  diverges at  $T = T_c/C$  when  $d \to 2$ , if  $T_c$  remains finite. Thus, we obtain an unphysical result unless the critical temperature  $T_c$  and, therefore,  $a(T_c/C)$  tend to zero at  $d \to 2$ .

On the other hand, it is a rigorously stated fact [29, 30] that the classical 2D XY model undergoes the Kosterlitz-Thouless phase transition at a finite temperature  $T_{\rm KT}$ . It means that a certain structural order without the spontaneous magnetization exists within the temperature region  $T < T_{\rm KT}$ . There is a general tendency of disordering with decreasing the spatial dimensionality d, and not vice versa. Thus, since the structural order exists at  $T < T_{\rm KT}$  and d = 2, some kind of order necessarily exists also at  $T < T_{\rm KT}$  and d > 2. Since the classical XY model undergoes the disorder  $\rightarrow$  long-range order phase transition at d > 2, this obviously is the long-range order. Thus, the critical temperature at  $d = 2 + \varepsilon$  is  $T_c \geq T_{\rm KT} \neq 0$  for an infinitesimal and positive  $\varepsilon$ , and it drops to zero by a jump at  $d = 2 - \varepsilon$ , as consistent with the rigorous consideration in [29].

The classical XY model belongs to the same universality class as the actual  $\varphi^4$  model at n=2, which means that both models become fully equivalent after a renormalization (a suitable renormalization will be discussed in Sec. 9.5). Thus,  $T_c$  does not vanish at  $d \to 2$  (for d > 2) also in the  $\varphi^4$  model. In such a way, the assumption  $G_{\perp}(\mathbf{k}) \simeq a(T) k^{-2}$  leads to a contradiction. In the stable region  $T < T_c/C$ , the Gaussian approximation  $G_{\perp}(\mathbf{k}) \simeq 1/(2ck^2)$  makes sense at finite not too small values of k. The above contradiction means that the Gaussian approximation with  $\lambda_{\perp} = 2$  cannot be extended to  $k \to 0$  in vicinity of d=2. The contradiction is removed only if  $\lambda_{\perp} < 2$  holds at  $d \to 2$  in the actual case of n=2.

It has been stated in [23, 25] that the essentially Gaussian result  $\lambda_{\perp}=2$  of the perturbative RG theory should be exact. However, some of the obtained "exact" results are rather unphysical. In particular, we find from Eq. (3.6) in [24] and from the formula  $\langle \pi^2 \rangle = -6A/u_0$  given in the line just below that

$$\langle \pi^2(\mathbf{x}) \rangle = (N-1) \int \frac{d^d q}{q^2}$$
 (53)

holds, where  $\pi(\mathbf{x})$  is the transverse (N-1)-component field which, in our notation, is composed of n-1 components labeled by index  $j \neq 1$ . Eq. (53) represents a senseless result, since  $\langle \pi^2(\mathbf{x}) \rangle$  given by this equation diverges at  $d \to 2$ . It is clear that  $\langle \pi^2(\mathbf{x}) \rangle$  cannot diverge in reality, as it follows from the Hamiltonian density (2.1) in [24] (Hamiltonian (1) in our paper): any field configuration with diverging  $\pi^2(\mathbf{x})$  provides a divergent  $\pi(\mathbf{x})$ -dependent term

$$\sim \frac{1}{2} |\nabla \pi(\mathbf{x})|^2 + \frac{u_0}{4!} (\pi^2(\mathbf{x}))^2$$
 (54)

in the Hamiltonian density and, therefore, gives no essential contribution to the statistical averages. The result (53) corresponds to a poor approximation where the second term in (54) is neglected. In a surprising way, based on Ward identities, authors of [24] and related papers have lost all the purely transverse diagrams, generated by the term  $\frac{u_0}{4!}(\pi^2(\mathbf{x}))^2$ , and stated that this is the exact result at  $r_0 \to -\infty$  as well as at  $k \to 0$ . According to [23, 24], the actual transverse term appears to be hidden in a shifted longitudinal field  $\bar{s}$ , which is considered as an independent Gaussian variable (cf. Eqs. (3.5) and (3.6) in [23]). Obviously, this is the fatal trivial error which leads to the above discussed unphysical result (53), since the determinant of the transformation Jacobian (from  $\pi$ , s to  $\pi$ ,  $\bar{s}$ ) is omitted in the relevant functional integrals. In this manner the  $\varphi^4$  model can be immediately reduced to the  $\varphi^2$  model by considering  $s = \varphi^2$  as a new variable! Including the Jacobian of the nonlinear transformation, the resulting model, however, remains non–Gaussian. Since (53) comes from

$$\langle \pi^2(\mathbf{x}) \rangle = (N-1) (2\pi)^{-d} \int G_{\perp}(\mathbf{k}) d^d k , \qquad (55)$$

the unphysical divergence of  $\langle \pi^2(\mathbf{x}) \rangle$  means that the predicted Gaussian form of the transverse correlation function  $G_{\perp}(\mathbf{k})$  is incorrect. Another aspect is that the method used in [23, 24] gives  $\lambda_{\perp} \equiv 2$  also at n=2 in contradiction with our previous discussion concerning the known rigorous results for the XY model.

Our consideration does not contradict the conventional statement (see [25] and references therein) that the Gaussian spin—wave theory [16] becomes exact at low temperatures, but only in the sense that it holds for any given nonzero  $\mathbf{k}$  at  $T \to 0$ , and in the limit  $\lim_{k\to 0} \lim_{t\to 0} \lim_{$ 

This problem persists in the classical treatment of the many–particle systems [15] which, in essence, is based on the Gaussian spin wave theory at  $T \to 0$ , as well as in the hydrodynamical description in [14], where the known results of the Gaussian spin wave theory [Eqs. (5.1a) and (5.1b)] have been implemented for a complete description. The treatment of [15], evidently, is not exact, since it breaks down at  $d \to 2$  for the two–component (n = 2) vector model (where  $T_c$  remains finite and we fix the temperature  $0 < T < T_c$ ) just like we have discussed already – the average  $\langle \pi^2(\mathbf{x}) \rangle$  is given by the integral (6.8) in [15] which diverges in this case (supposed  $(2\pi)^{-3}d^3k \to (2\pi)^{-d}d^dk$ ).

A slightly different perturbative RG approach has been developed in [21] to analyze the nonlinear  $\sigma$  model. In this case the modulus of  $\varphi(\mathbf{x})$  is fixed which automatically removes the divergence of  $\langle \pi^2(\mathbf{x}) \rangle$ . A finite external field h has been introduced there to make an expansion. The correlation functions have the power–like singularities of interest only at h = +0, which means that in this case we have to consider the limit  $\lim_{k\to 0} \lim_{h\to 0} i$ . i. e., the limit  $h\to 0$  must be taken first at a fixed nonzero k (p in formulae used in [21]). The results in [21] are not rigorous since the expansions used there are purely formal, i. e.,

they break down in this limit. Besides, contrary to the approximations in [21], it should be clear that the exact renormalization is a rather nontrivial problem which cannot be reduced to a finding of only two renormalization constants. If, e. g., we make a real–space renormalization of the Heisenberg model, say, with the scaling factor s=2, then the statistically averaged block–spins of the Kadanoff transformation (composed of  $s^d$  original spins) do not have a fixed modulus – simply the original model does not include the constraint  $|\varphi(\mathbf{x})| = const$  for the block averages. It means that the transformation with any finite s yields a Hamiltonian of form different from the original one, i. e., the original Hamiltonian with merely renormalized coupling constant can never be the fixed–point Hamiltonian.

Another approach, which is based on effective Lagrangians, has been developed in [28]. However, due to several rough (fatal) errors in Sec. 3 of this paper we cannot appreciate the basic results. For example, we have found that the transformation

$$v_{\mu}^{\Omega} = \Omega v_{\mu} \Omega^{-1} , \qquad \vec{H}^{\Omega} = \Omega \vec{H}$$
 (56)

brings the Lagrangian

$$\mathcal{L} = \frac{1}{2} D_{\mu} \vec{\phi} D_{\mu} \vec{\phi} + \frac{1}{2} m^2 \vec{\phi} \vec{\phi} + \frac{1}{4} \lambda (\vec{\phi} \vec{\phi})^2 - \vec{H} \vec{\phi}$$
 (57)

with

$$D_{\mu}\vec{\phi}(\mathbf{x}) = \partial_{\mu}\vec{\phi}(\mathbf{x}) + v_{\mu}(\mathbf{x})\vec{\phi}(\mathbf{x})$$
(58)

back to its original form after a space–independent rotation  $\Omega$ . Namely,

$$\mathcal{L}\left(v_{\mu}^{\Omega}, \vec{H}^{\Omega}, \Omega \vec{\phi}\right) = \mathcal{L}\left(v_{\mu}, \vec{H}, \vec{\phi}\right) \tag{59}$$

holds, as it can be verified by a simple substitution taking into account that  $\Omega \vec{A} \, \Omega \vec{B} = \vec{A} \vec{B}$  holds for any vectors  $\vec{A}$  and  $\vec{B}$ , since the rotation of the coordinate system does not change the scalar product, as well as that  $\partial_{\mu}\Omega\vec{\phi} = \Omega\,\partial_{\mu}\vec{\phi}$  obviously is true for a space–independent matrix  $\Omega$ . As a consequence, the partition functions obey the equation

$$Z\left(v_{\mu}^{\Omega}, \vec{H}^{\Omega}\right) = Z\left(v_{\mu}, \vec{H}\right) \tag{60}$$

with  $v^{\Omega}_{\mu}$  and  $\vec{H}^{\Omega}$  defined in (56). But Eq. (3.7) in [28] disagrees with (56): it contains an odd term  $\Omega \partial_{\mu} \Omega^{-1}$  which reduces to  $\partial_{\mu}$  in the case of space—independent  $\Omega$ . The following relevant equations on page 247 contain similar errors, i. e., it is easy to verify that they do not hold in the simplest case of a space—independent rotation. Some numerical support of this theory can be found in literature [32, 33], where a finite—size scaling within a transient region of very small fields comparable with  $L^{-3}$  (where L is the linear size of 3D lattice) have been considered. Our theoretical predictions, however, refer to the limit  $\lim_{h\to 0} \lim_{L\to\infty}$ , therefore the tests made in [32, 33] are of little interest here.

Concluding this subsection, it is worthy to mention that the experimental measurements of susceptibility  $\chi$  depending on field h in isotropous ferromagnets like high–purity polycrystalline Ni [34] are incompatible with the conventional RG prediction  $\chi \sim h^{(d-4)/2}$ . Moreover, our Monte Carlo results for 3D XY model discussed in Sec. 10 are incompatible with this prediction, as well. Thus, according to the given theoretical arguments, the conventional claims that the Gaussian approximation is asymptotically exact at  $k \to 0$  simply cannot be correct, and there exist also numerical evidences for this.

#### 9.2 The leading asymptotic behavior

Let us now discuss the solution below  $T_c$  at small wave vectors  $k \to 0$  within our diagrammatic approach. By analyzing several possibilities we have arrived to a conclusion that the true physical asymptotic solution for 2 < d < 4 and n > 1 is

$$G_{\perp}(\mathbf{k}) \simeq a \, k^{-\lambda_{\perp}} \,, \qquad G_{\parallel}(\mathbf{k}) \simeq b \, k^{-\lambda_{\parallel}}$$
 (61)

whith some amplitudes a and b, and exponents

$$d/2 < \lambda_{\perp} < 2$$
 and  $\lambda_{\parallel} = 2\lambda_{\perp} - d$ . (62)

Only in this case the exponents on the left hand side of equation (6) for  $1/G_i(\mathbf{k})$  coincide with those on the right hand side, if calculated by the method developed in [5] for the case  $T = T_c$ . Besides, only at  $d/2 < \lambda_{\perp} < 2$  we arrive to a solution which coincides both with the scaling hypothesis (31) and general renormalization group arguments discussed further in Sec. 9.5.

Below we show that (61) and (62) really represent a selfconsistent solution of our equations. According to (62),  $\lambda_{\parallel} > 0$  holds, so that  $G_{\parallel}(\mathbf{k})$  diverges at  $k \to 0$ . Thus, we have  $1/G_{\parallel}(+0) = 0$ . Eq. (47) then implies that  $R_{\parallel}(+0) = R_{\parallel}(\mathbf{0})$ . The latter relation always is true for the transverse components, as already discussed in Sec. 8. Our analysis is based on Eq. (46), which at these conditions reduces to

$$1/(2G_i(\mathbf{k})) = ck^2 + R_i(\mathbf{k}) - R_i(\mathbf{0}).$$
(63)

First let us consider only the "normal" contributions without the zero-vector-cumulant insertions, as explained in Sec. 7 and Appendix. In this case (at the condition (62)), the main terms in the asymptotic expansion of  $\Sigma(\mathbf{q},\zeta)$  (at  $\mathbf{q}\neq\mathbf{0}$  for any given  $\Lambda/q$  considered as independent variable) are represented by partial contributions, coming from all diagrams in (11), where either all  $N_j$  solid lines of the j-th diagram are associated with the transverse components  $G_{\perp}(\mathbf{k})$ , or m of  $2m \leq N_j$  solid lines which are associated with  $G_{\parallel}(\mathbf{k})$  have zero wave vector. It is true at 2 < d < 4 and (62), since other terms provide only small corrections, as discussed further in Sec. 9.3. Since  $1/\Sigma(\mathbf{0},\zeta)=0$  holds at  $V=\infty$ , only those configurations give a nonvanishing contribution where nonzero wave vectors are related to the waved lines. Therefore also maximally one half of all lines associated with the longitudinal component i=1 can have zero wave vector, as regards the nonvanishing (at  $V\to\infty$ ) terms related to  $\Sigma(\mathbf{q},\zeta)$  with  $\mathbf{q}\neq\mathbf{0}$ . This holds because solid lines make closed loops and maximally each second line of a loop can have zero wave vector, provided that all waved and dashed lines, connected to this loop, have nonzero wave vectors.

It is suitable to represent the amplitude b in (61) as  $b = b' \cdot a^2/M^2$ . Then, by normalizing all wave vectors to the current value of q, we find that the selfconsistent solution of (13) has the scaled form

$$\Sigma(\mathbf{q},\zeta) = a^2 q^{d-2\lambda_{\perp}} \psi\left(\Lambda/q,\zeta,\lambda_{\perp},b',u,d,n\right)$$
(64)

which is proven by the method described in detail in [5], taking into account all diagrams of (11) and only the main terms of the asymptotic expansion at  $k \to 0$ . These are the partial contributions discussed in the paragraph above. It is supposed also that term "1"

in (12), providing a small corection at  $\lambda_{\parallel} > 0$ , is neglected. In the same manner, by normalizing all wave vectors to the current value of k, we arrive to the scaled form

$$\partial \Sigma(\mathbf{q},\zeta)/\partial G_{j}(\mathbf{k}) = V^{-1}ak^{-\lambda_{\perp}}Y_{\perp}(\mathbf{q}/k,\Lambda/k,\zeta,\lambda_{\perp},b',u,d,n) : j \neq 1$$

$$\partial \Sigma(\mathbf{q},\zeta)/\partial G_{1}(\mathbf{k}) = V^{-1}M^{2}k^{-d}Y_{\parallel}(\mathbf{q}/k,\Lambda/k,\zeta,\lambda_{\perp},b',u,d,n)$$

$$+ \delta_{\mathbf{q},\mathbf{k}}M^{2}\hat{Y}_{\parallel}(\mathbf{q}/k,\Lambda/k,\zeta,\lambda_{\perp},b',u,d,n) ,$$
(66)

where the term with Kronecker's symbol appears due to the extraordinary contributions discussed in Sec. 8. By virtue of (65), (66), and (8), (39) we obtain also

$$R_{\perp}(\mathbf{k}) = a^{-1}k^{\lambda_{\perp}} \bar{\phi}_{\perp} (\Lambda/k, \lambda_{\perp}, b', u, d, n)$$
(67)

$$R_{\parallel}(\mathbf{k}) = b^{-1}k^{\lambda_{\parallel}} \bar{\phi}_{\parallel} \left( \Lambda/k, \lambda_{\perp}, b', u, d, n \right) . \tag{68}$$

The fact that  $R_{\perp}(\mathbf{0})$  is constant means that there exists the limit  $\lim_{k\to 0} R_{\perp}(\mathbf{k}) = R_{\perp}(\mathbf{0})$ , which, according to (67), implies that  $a\Lambda^{-\lambda_{\perp}}R_{\perp}(\mathbf{0})$  does not depend on a and  $\Lambda$  and thus the scaling function  $\bar{\phi}$  can be represented as

$$\bar{\phi}_{\perp} \left( \Lambda/k, \lambda_{\perp}, b', u, d, n \right) = a \Lambda^{-\lambda_{\perp}} R_{\perp}(\mathbf{0}) \cdot (\Lambda/k)^{\lambda_{\perp}} + 1/\left[ 2\phi_{\perp} \left( \Lambda/k, \lambda_{\perp}, b', u, d, n \right) \right]$$
(69)

with another scaling function  $\phi_{\perp}$  instead of  $\bar{\phi}_{\perp}$ . Analogous equation for  $\bar{\phi}_{\parallel}$  reads

$$\bar{\phi}_{\parallel} \left( \Lambda/k, \lambda_{\perp}, b', u, d, n \right) = b \Lambda^{-\lambda_{\parallel}} R_{\parallel}(\mathbf{0}) \cdot (\Lambda/k)^{\lambda_{\parallel}} + 1/\left[ 2\phi_{\parallel} \left( \Lambda/k, \lambda_{\perp}, b', u, d, n \right) \right] . \tag{70}$$

Note that we always consider  $\lambda_{\perp}$ , but not  $\lambda_{\parallel}$ , as an independent argument, therefore some asymmetry appears in formulae. By substituting Eqs. (67) to (70) and (61) into (63), and neglecting the correction term  $ck^2$ , we obtain

$$G_{\perp}(\mathbf{k}) = a k^{-\lambda_{\perp}} = a \phi_{\perp} (\Lambda/k, \lambda_{\perp}, b', u, d, n) k^{-\lambda_{\perp}}$$
(71)

$$G_{\parallel}(\mathbf{k}) = b k^{-\lambda_{\parallel}} = b \phi_{\parallel} (\Lambda/k, \lambda_{\perp}, b', u, d, n) k^{-\lambda_{\parallel}}. \tag{72}$$

Up to now we have neglected the zero–vector–cumulant insertions in the derivation of Eqs. (71) and (72). However, following the method in Appendix, these insertions can only renormalize the scaling functions  $\phi_{\perp}$  and  $\phi_{\parallel}$ , so that Eqs. (71) and (72) hold.

As discussed in Sec. 6, the limit  $u \to 0$  with simultaneous tending of k to zero like  $k \sim u^r k_{crit}(u)$  (where r > 0) has to be considered to ensure correct critical exponents. The existence of the solution for (71) and (72) implies the existence of the corresponding limits for  $\phi_{\perp}$  and  $\phi_{\parallel}$ . Note that these functions do not contain u-dependent factors in our scaling analysis (which is true also for  $\phi$  in Eq. (42) of [5]), and only weak u-dependence (at  $u \to 0$ ) can be induced by the integration limits in (13). Thus, Eqs. (71) and (72) yield

$$\lim_{u \to 0} \phi_{\perp} \left( \Lambda u^{-r} k_{crit}^{-1}(u), \lambda_{\perp}, b', u, d, n \right) = B_{\perp} \left( \lambda_{\perp}, b', d, n \right) = 1 \tag{73}$$

$$\lim_{u \to 0} \phi_{\parallel} \left( \Lambda u^{-r} k_{crit}^{-1}(u), \lambda_{\perp}, b', u, d, n \right) = B_{\parallel} \left( \lambda_{\perp}, b', d, n \right) = 1.$$
 (74)

Eqs. (73) and (74) can be, in principle, solved with respect to  $\lambda_{\perp}$  and b'. It follows herefrom that not only the exponent  $\lambda_{\perp}$ , but also the quantity  $b' = bM^2/a^2$  is universal, i. e., dependent only on the spatial dimensionality d and dimensionality of the order parameter n. In general, no universality of amplitudes is expected, so that the latter rather surprising conclusion refers only to the actual limit  $u \to 0$ . Nevertheless, the universality of  $bM^2/a^2$  coincides with some general non–perturbative renormalization group arguments discussed in Sec. 9.5, which show that the restriction to small u values is purely formal.

#### 9.3 Corrections to scaling

In Sec. 9.2 we have considered only the dominant terms in the asymptotic solution at  $k \to 0$ . Now we shall discuss corrections to scaling. There are following sources of corrections.

- (i) Since  $R_{\perp}(\mathbf{k}) R_{\perp}(\mathbf{0}) \propto a^{-1}k^{\lambda_{\perp}}$  and  $\lambda_{\perp} < 2$  hold, the term  $ck^2$  in Eq. (63) for the transverse components  $i \neq 1$  produces a correction which is by factor  $\varepsilon_1(k) \propto a k^{2-\lambda_{\perp}}$  smaller than the main term at  $k \to 0$ . In analogy, a correction  $\varepsilon'_1(k) \propto b k^{2-\lambda_{\parallel}}$  is generated in the same equation for i = 1.
- (ii) According to (64) and (62), at any given  $\Lambda/q$ , the term "1" in Eq. (12) represents a small correction  $\propto a^{-2}q^{\lambda_{\parallel}}$  to the amplitude of the main term. Finally, it generates an amplitude correction  $\varepsilon_2(k) \propto a^{-2}k^{\lambda_{\parallel}}$  in the asymptotic expansion of  $G(\mathbf{k})$ .
- (iii) Consider partial contributions to  $\Sigma(\mathbf{q},\zeta)$ , coming from all diagrams in (11), where less than one half of the solid lines which belong to loops with i=1 have zero wave vector. As compared to the dominant contributions discussed in Sec. 9.2, they generate small corrections represented by an expansion in terms of  $\varepsilon_3(k)$ , where  $\varepsilon_3(k) \propto (b/a) k^{\lambda_{\perp} \lambda_{\parallel}}$  corresponds to a replacement of  $G_{\perp}(\mathbf{k})$  with  $G_{\parallel}(\mathbf{k})$  for one solid line with nonzero wave vector.

Note that the corrections  $\varepsilon_{\ell}(k)$  are small at  $k \to 0$  only for  $d/2 < \lambda_{\perp} < 2$ , so that our analysis cannot be formally extended outside of this interval. We have included an explicit dependence of  $\varepsilon_{\ell}(k)$  on the amplitudes a and b, since their singular behavior is relevant for joining of the asymptotic solutions at  $T \to T_c$ . Since  $\varepsilon'_1(k) \propto \varepsilon_1(k) \varepsilon_3(k)$  holds, we have no more than three independent correction sources.

The expansion in powers of  $\varepsilon_{\ell}(k)$  is a companied by scaling functions depending on  $\Lambda/k$ . Like in (73) and (74), these scaling functions can be replaced by amplitudes which are independent of k, when considering the limit  $u \to 0$  and  $k \sim u^r k_{crit}(u)$ . This replacement is analogous to that at  $T = T_c$  and has the same motivation [5]. It results in the asymptotic expansion for the Greens function

$$G_i(\mathbf{k}) = \sum_{\ell \ge 0} b_i(\ell) k^{-\lambda_i(\ell)} , \qquad (75)$$

where relations  $\lambda_i(0) \equiv \lambda_{\parallel}$ ,  $b_i(0) \equiv b$  hold for i = 1, and  $\lambda_i(0) \equiv \lambda_{\perp}$ ,  $b_i(0) \equiv a$  – for  $i \neq 1$ . A term with  $\ell \geq 1$  represents a correction of order  $\varepsilon_1^{n_1(\ell)} \varepsilon_2^{n_2(\ell)} \varepsilon_3^{n_3(\ell)}$  with the exponent

$$\lambda_i(\ell) = \lambda_i(0) - n_1(\ell) \cdot (2 - \lambda_{\perp}) - n_2(\ell) \cdot \lambda_{\parallel} - n_3(\ell) \cdot (\lambda_{\perp} - \lambda_{\parallel}), \qquad (76)$$

where  $n_j(\ell) \geq 0$  are integer numbers such that  $\sum_j n_j(\ell) \geq 1$ . Note that we always allow a possibility that some of the expansion coefficients, in this case some of  $b_i(\ell)$ , are zero. The expansion in powers of  $\varepsilon_2(k) \propto k^{4-d}$  and  $\varepsilon_3(k) \propto k^{d-2}$ , proposed by the perturbative RG theory [22, 23], is recovered by formally setting  $\lambda_{\perp} = 2$ .

#### 9.4 Joining of asymptotic solutions

Consider now how our expansion (75) coincides with (31) and (50) when approaching the critical point. Retaining only the leading terms, the consistency is ensured if the scaling

functions of the dominant terms behave as  $g_{\perp}(z) \propto z^{-\lambda_{\perp}}$  (for  $i \neq 1$ ) and  $g_{\parallel}(z) \propto z^{-\lambda_{\parallel}}$  (for i = 1) at  $z \to 0$ , and  $a \propto \hat{\xi}^{\lambda - \lambda_{\perp}}$ ,  $b \propto \hat{\xi}^{\lambda - \lambda_{\parallel}}$  hold for the amplitudes in (61) at  $\Delta \to 0$ , where  $\lambda = \gamma/\nu = 2 - \eta$ . Here  $\hat{\xi} = \Delta^{-\nu}$  is an analog of the correlation length. This is a property of the solution exceptionally at  $d/2 < \lambda_{\perp} < 2$  that the consideration of the long-wave limit does not provide any constraint for the amplitude a in (71), whereas the other amplitude b is related to a via  $b = b' \cdot a^2/M^2$ . Taking into account the scaling law (48), the relations  $a \propto \hat{\xi}^{\lambda - \lambda_{\parallel}}$  and  $b \propto \hat{\xi}^{\lambda - \lambda_{\parallel}}$  mean that  $bM^2/a^2$  is constant at  $\Delta \to 0$ . It is consistent with the statement in Sec. 9.2 that b' = const at  $u \to 0$  for any  $T < T_c$ .

The expansion (50) with the exponents  $\gamma_{\ell}$  (51) completely agree with (75) and (76) provided that the scaling functions have an asymptotic expansion

$$g_i^{(\ell)}(z) = \sum_{\ell>0} B_i^{(\ell)} z^{-\lambda_i(\ell)}$$
 (77)

at  $z \to 0$ . In this case the amplitudes  $b_i(\ell) \sim \Delta^{-\gamma + \gamma_\ell + \nu \lambda_i(\ell)}$  have corrections to scaling where the main term is multiplied by  $\propto \Delta^{\gamma_m}$ .

#### 9.5 Non-perturbative renormalization group arguments

The relation  $\lambda_{\parallel}=2\lambda_{\perp}-d$  as well as the universality of the ratio  $bM^2/a^2$  have a simple interpretation in view of some renormalization group (RG) analysis. Our  $\varphi^4$  model can be formulated on a discrete lattice, representing the gradient term by finite differences. At h=+0, we consider the transformation consisting of

- (i) Kadanoff transformation replacing single lattice spins by block–spins, where each block–spin is an average over  $s^d$  spins;
- (ii) shrinkage of the new lattice s times to return to the initial lattice constant. In distinction to the standard renormalization, we do not rescale the field  $\varphi$ .

The distribution over block-spins is described by new Hamiltonian  $T_sH$ , where the notation  $T_s$  is used to distinguish from the standard RG transformation  $R_s$ . The Kadanoff transformation does not change neither the magnetization nor the long-distance behavior of the real–space Greens functions  $\widetilde{G}_{\perp}(\mathbf{x}) = \langle \varphi_i(\mathbf{x}_1) \varphi_i(\mathbf{x}_1 + \mathbf{x}) \rangle = \hat{a}x^{\lambda_{\perp} - d} \ (i \neq 1)$  and  $\widetilde{G}_{\parallel}(\mathbf{x}) = \langle \varphi_1(\mathbf{x}_1) \varphi_1(\mathbf{x}_1 + \mathbf{x}) \rangle - M^2 = \hat{b}x^{\lambda_{\parallel} - d} \ \text{at} \ x \to \infty$ , where  $\hat{a} = c_a \cdot a$  and  $\hat{b} = c_b \cdot b$  are the amplitudes. The proportionality coefficients  $c_a$  and  $c_b$  are universal, since  $G_{\perp}(\mathbf{k}) \simeq a \, k^{-\lambda_{\perp}}$  and  $G_{\parallel}(\mathbf{k}) \simeq b \, k^{-\lambda_{\parallel}}$  are the Fourier transforms of  $\widetilde{G}_{\perp}(\mathbf{x})$  and  $\widetilde{G}_{\parallel}(\mathbf{x})$ , respectively. Taking into account the shrinkage of the lattice at step (ii), magnetization Mis invariant of the transformation  $T_s$ , whereas the amplitudes rescale as  $\hat{a}(s) = \hat{a}(1) \cdot s^{\lambda_{\perp} - d}$ and  $\hat{b}(s) = \hat{b}(1) \cdot s^{\lambda_{\parallel} - d}$ . The modulus conservation principle is true at large renormalization scales s, since the variation of average modulus for large blocks of spins is related to a much greater increase in the systems energy as compared to a gradual long-wave perturbation of spin orientation. The validity of this principle is restricted by the condition that the mean amplitude of the relative fluctuation of the modulus has to be much smaller than the mean squared fluctuation of the orientation angle for the block-spins of the Kadanoff transformation. The non-perturbative renormalization group arguments given below are in agreement with our foregoing diagrammatic analysis, assuming that this condition is fulfilled for large s in the actual case of 2 < d < 4. Thus, the renormalized Hamiltonian

can be written as

$$T_s(H/T) \simeq \sum_{\mathbf{x}} \left[ \frac{1}{|\delta(|\varphi(\mathbf{x})| - \varphi_0)|} + Q\left\{ \hat{a}^{-1/2}(s) \varphi_{\perp}(\mathbf{x}) \right\} \right]$$
(78)

at  $s \to \infty$ , where the first term represents the modulus conservation principle allowing only those configurations with non-diverging Hamiltonian where  $|\varphi(\mathbf{x})| = \varphi_0$ , and Q is some functional of the configuration of the transverse order parameter (n-1 component vector) field  $\varphi_{\perp}(\mathbf{x})$ . In this case only the infinitely small (at  $s \to \infty$ ) transverse components  $\varphi_i(\mathbf{x})$  with  $i \neq 1$  are independent variables, since

$$\varphi_0 - \varphi_1(\mathbf{x}) \simeq \sum_{i=2}^n \varphi_i^2(\mathbf{x})/(2M)$$
 (79)

holds according to  $|\varphi(\mathbf{x})| = \varphi_0$ . Not loosing the generality, we have considered the spatial configuration of the normalized transverse components  $\hat{a}^{-1/2}(s) \varphi_{\perp}(\mathbf{x})$  as an argument of the functional Q. According to the definition of  $\widetilde{G}_{\perp}(\mathbf{x})$ , the function  $f_{\perp}(\mathbf{x}) = \left\langle \hat{a}^{-1/2}(s) \varphi_i(\mathbf{x}_1) \cdot \hat{a}^{-1/2}(s) \varphi_i(\mathbf{x}_1 + \mathbf{x}) \right\rangle = \hat{a}^{-1}(s) \widetilde{G}_{\perp}(\mathbf{x})$  with  $i \neq 1$  has a universal asymptotic behavior  $f_{\perp}(\mathbf{x}) = x^{\lambda_{\perp} - d}$  at  $x \to \infty$ . Since this average is composed of arguments of Q, the sufficient condition for its universal asymptotic behavior is the universality of the functional  $Q\{z(\mathbf{x})\}$ . The latter is consistent with the idea that the transformation of Q (assuming that at any s the transformed Hamiltonian can be approximated by (78) according to some a priori defined criterion) has a fixed point

$$Q^*\{z(\mathbf{x})\} = \lim_{s \to \infty} T_s Q\{z(\mathbf{x})\}$$
(80)

which, however, may be different for each universality class. In the conventional RG transformation  $R_s$  the field would be rescaled as  $\varphi_{\perp}(\mathbf{x})s^{(d-\lambda_{\perp})/2} \Rightarrow \varphi_{\perp}(\mathbf{x})$ , so that Q in (78) would contain no explicit scaling factor s. Nevertheless, we prefer our notation, since it is suited to express the modulus conservation principle. Accepting (80), any statistical average composed of arguments  $\hat{a}^{-1/2}(s)\,\varphi_{\perp}(\mathbf{x})$  is universal at  $s\to\infty$ . In particular,  $f_{\parallel}(\mathbf{x}) = \left\langle \left(\hat{a}^{-1/2}(s)\,\varphi_i(\mathbf{x}_1)\right)^2 \cdot \left(\hat{a}^{-1/2}(s)\,\varphi_i(\mathbf{x}_1+\mathbf{x})\right)^2 \right\rangle$  with  $i\neq 1$  is a universal function. According to (79), we have  $\tilde{G}_{\parallel}(\mathbf{x}) = \hat{b}(s)x^{\lambda_{\parallel}-d} = (n-1)(2M)^{-2}\hat{a}^2(s)\left[f_{\parallel}(\mathbf{x}) - f_{\parallel}(\infty)\right]$  at  $x\to\infty$  and  $s\to\infty$ . The universality of  $f_{\parallel}(\mathbf{x})$  then implies that  $\hat{b}(s)M^2/\hat{a}^2(s)$  must be universal at  $s\to\infty$ . According to the scaling rules  $\hat{a}(s)=\hat{a}(1)\cdot s^{\lambda_{\perp}-d}$  and  $\hat{b}(s)=\hat{b}(1)\cdot s^{\lambda_{\parallel}-d}$ , the latter is possible only if  $\lambda_{\parallel}=2\lambda_{\perp}-d$  holds, whence it follows also that  $\hat{b}(1)M^2/\hat{a}^2(1)$  and  $b(1)M^2/a^2(1)\equiv bM^2/a^2$  are universal, i.e., dependent merely on n and d. Thus we recover one of relations (62), as well as the universality of the ratio  $bM^2/a^2$  discussed in Sec. 9.2.

It is very likely that the accuracy of (78) is limited even at  $s \to \infty$ . However, there exists a less constrained form

$$T_s(H/T) = \sum_{\mathbf{x}} Q\left\{ (M - \varphi_1(\mathbf{x})) \, M \hat{a}^{-1}(s), \, \hat{a}^{-1/2}(s) \, \varphi_{\perp}(\mathbf{x}) \right\}$$
(81)

for the renormalized Hamiltonian at  $s \to \infty$ , as consistent with the idea that Eq. (79) with  $\varphi_0 = M + \mathcal{O}\left(\varphi_\perp^2/M\right)$  holds approximately for relevant configurations of block–spins. It also leads to the relation  $\lambda_{\parallel} = 2\lambda_{\perp} - d$  and the universality of  $bM^2/a^2$ .

Contrary to the previous discussion in Sec. 9.2, in this case our conclusions are not restricted to small u.

#### 9.6 Magnetization in a small external field

Here we discuss the qualitative behavior of magnetization M in a small external field.

The modulus conservation principle holds far below the critical point (at large negative  $r_0$ ) where the fluctuations of modulus  $|\varphi(\mathbf{x})|$  are reduced to a small vicinity of  $\varphi_0(h) \simeq \sqrt{-r_0/(2u)} - h/(4r_0)$ , as consistent with the minimum of Hamiltonian (1). In this case we have

$$M(h) = \langle \varphi_1(\mathbf{x}) \rangle \simeq \varphi_0(h) \left( 1 - \frac{1}{2} \left\langle \theta^2(\mathbf{x}) \right\rangle(h) \right) ,$$
 (82)

where  $\theta(\mathbf{x})$  is the angular deviation of  $\varphi(\mathbf{x})$  from the direction of the external field  $\mathbf{h}$ . We consider the limit  $\lim_{c\to\infty}\lim_{r_0\to-\infty}\lim_{h\to 0}$  where Eq. (82) is asymptotically exact, since  $|\varphi(\mathbf{x})| = const$  holds with an unlimited accuracy and, simultaneously, the angular fluctuations are suppressed. The variation of  $\varphi_0(h)$  with h is analytical, whereas the singular behavior of M(h) at  $h\to 0$  is due to the term

$$\left\langle \theta^2(\mathbf{x}) \right\rangle(h) \sim \widetilde{G}_{\perp}(\mathbf{0}) = (2\pi)^{-d} \int G_{\perp}(\mathbf{k}) \, d\mathbf{k} .$$
 (83)

The transverse correlation function behaves like  $G_{\perp}(\mathbf{k}) \simeq a \, k^{-\lambda_{\perp}}$  (the  $k \to 0$  asymptotic at h = 0) when k is decreased below some  $k_{crit}$  (defined for any given  $r_0$  and c) if  $h \to 0$  until it saturates at the known value M/h valid for  $\mathbf{k} = \mathbf{0}$ . From this we find

$$M(h) - M(+0) \propto h^{(d/\lambda_{\perp})-1}$$
 at  $h \to 0$ . (84)

Since the exponent  $\rho = (d/\lambda_{\perp}) - 1$  is universal, Eq. (84) is valid for any  $T < T_c$  including vicinity of the critical point. This yields the longitudinal susceptibility

$$\chi_{\parallel} = \partial M(h)/\partial h \propto h^{(d-2\lambda_{\perp})/\lambda_{\perp}} = h^{-\lambda_{\parallel}/\lambda_{\perp}} \quad \text{at} \quad h \to 0 .$$
 (85)

According to (62), we have  $(d/2)-1 < \rho < 1$ , which yields  $1/2 < \rho < 1$  in three dimensions. The lower value  $\rho = 0.5$  corresponds to the conventional statement [13, 17, 24] that  $\lambda_{\perp} = 2$ . Our numerical test in the following section, however, does not support this possibility.

#### 10 Monte Carlo test in 3D XY model

To verify the theoretical predictions for the exponent  $\rho = (d/\lambda_{\perp}) - 1$  in (84), we have made Monte Carlo (MC) simulations of 3D XY model on simple cubic lattice with the Hamiltonian

$$\frac{H}{T} = -K \left( \sum_{\langle ij \rangle} \mathbf{s}_i \mathbf{s}_j + \sum_i \mathbf{h} \mathbf{s}_i \right) , \qquad (86)$$

where  $\mathbf{s}_i$  is the spin variable (two-component vector) of the *i*-th lattice site, K is the coupling constant, and  $\mathbf{h}$  is the external field. Based on the universality argument (cf. Sec. 9.5), the same value of  $\rho$  is valid also for the actual  $\varphi^4$  model with two-dimensional order parameter (n=2). The simulations have been made in the ordered phase at  $K=0.475, 0.5, 0.55 > K_c$ , where  $K_c \simeq 0.4542$  [9] is the critical point. Only the case K=0.5 is discussed in detail, since the analysis made at K=0.475 and K=0.55 is similar. The quatity  $\langle |m| \rangle$ , where m is the magnetization per spin, has been evaluated for different linear sizes of the lattice L. The Wolff's cluster algorithm [35] has been used at

Table 1: The MC simulated values of  $\langle |m| \rangle$  for 3D XY model depending on the external field at a fixed coupling constant K = 0.5.

	$\langle \mid m \mid \rangle$			
h	L=8	L=16	L=32	L=64
0.028	0.586155(85)	0.567394(63)	0.562201(78)	0.561218(45)
0.04	0.593381(86)	0.576368(91)	0.572118(70)	0.571425(55)
0.056	0.601719(100)	0.586635(99)	0.583529(77)	0.583020(45)
0.08	0.613203(93)	0.600377(109)	0.597872(63)	0.597552(52)
0.112	0.626239(89)	0.615581(81)	0.613741(61)	0.613527(46)
0.16	0.643071(78)	0.634658(63)	0.633304(50)	0.633242(31)
0.224	0.661554(58)	0.655097(58)	0.654166(34)	0.654016(28)
0.32	0.684105(62)	0.679169(51)	0.678533(31)	0.678483(22)
0.448	0.707654(44)	0.704018(37)	0.703606(32)	0.703496(20)
0.64	0.734667(38)	0.732058(25)	0.731754(22)	0.731714(16)

h=0. The results are  $\langle \mid m \mid \rangle = 0.570297(23),\ 0.542411(21),\ 0.530317(20),\ 0.524606(19),\ 0.521846(26),\ and\ 0.520449(35)$  for  $L=8,\ 16,\ 32,\ 64,\ 128,\ and\ 256,\ respectively.$  These values for L=8 to 256 have been obtained by an averaging over, respectively,  $8\cdot 10^7,\ 2\cdot 10^7,\ 5\cdot 10^6,\ 1.25\cdot 10^6,\ 3.125\cdot 10^5,\ and\ 7.5\cdot 10^4$  cluster algorithm steps. Each simulation has been split typically in 51 bins to calculate the mean value and the standard deviation discarding the first bin (first 2 bins at L=256). The value at L=256 has been obtained by a weighted averaging over two simulations including totally 30 (10+20) not discarded bins, each consisting of 2500 cluster updates.

The simulations at h>0 have been done by the Metropolis algorithm. The results of simulation for L=8, 16, 32 and 64 are listed in Tab. 1. The statistical averages have been evaluated from  $3.2 \cdot 10^6 \times (64/L^2)$  sweeps at  $0.08 \le h \le 0.64$ , discarding no less than 50 000 sweeps from the beginning of the simulation to ensure an accurate equilibration. The total length of the simulation as well as the discarded part have been increased by a factor 0.08/h at h < 0.08. Like in the case of h=0, each simulation has been split in bins, using the last 50 ones for the estimations.

The linear congruatial generator with multiplier  $7^5$  and modulo  $2^{31} - 1$  (Lewis generator), improved by a shuffling, has been used as a source of pseudo random numbers. The standard shuffling scheme [36] with the length of string  $N = 10^6$  has been completed by a second shuffling, where the whole cycle (consisting of  $2^{31} - 2$  numbers) of the original generator has been split in  $2^{20}$  segments, restarting the generation from the beginning of a new randomly choosen segment when the previous one is exhausted. The scheme provided excellent results in test simulations of 2D Ising model, where the simulated values of internal energy, specific heat  $C_V$ , and its first two derivatives have been compared with the exact results. No systematic deviations have been observed in rather long simulations at the critical point providing the standard error in  $C_V$  as small as 0.02% for  $48 \times 48$  lattice and 0.11% for  $256 \times 256$  lattice.

The quantity M(+0) in (84) has been evaluated by extrapolating our  $\langle |m| \rangle$  data to the thermodynamic limit, based on an empirical observation that  $\langle |m| \rangle$  is almost linear

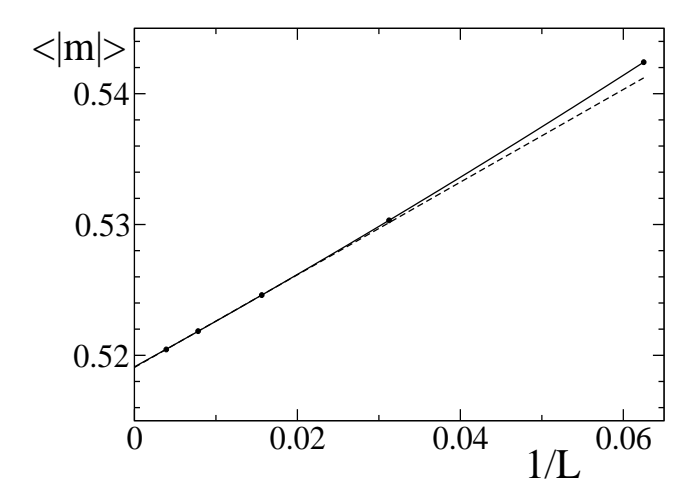


Figure 1: The mean magnetization modulus  $\langle |m| \rangle$  vs the inverse linear system size 1/L at  $K=0.5,\ h=0$ . The statistical errors are much smaller than the symbol size. The linear extrapolation (dashed line) and the quadratic fit (solid line) yield the asymptotic values 0.519073(37) and 0.519116(30), respectively.

function of the inverse lattice size 1/L, as it is evident from Fig. 1. The linear fit of three largest sizes (dashed line in Fig. 1) provides M(+0) = 0.519073(37), the quadratic fit within  $16 \le L \le 256$  yields M(+0) = 0.519116(30) (solid line), whereas the cubic fit within  $8 \le L \le 256$  gives us M(+0) = 0.519096(33). The values of goodness Q (see [37] for the definition) of the respective fits are 0.769, 0.767, and 0.794. We have accepted the result M(+0) = 0.519116(30) of the quadratic fit for our further estimations, although we could choose any of two other values as well, since the differences are rather small. Moreover, even a shift by 20 standard deviations would not change the qualitative picture in Fig. 2, where the effective critical exponent  $\rho_{eff}(h,L)$  is shown, defined as the mean slope of the  $\ln[M(h',L) - M(+0)]$  vs  $\ln h'$  plot within  $h' \in [h,2h]$ , where M(h',L) is the value of  $\langle |m| \rangle$  at the field h' and the linear lattice size L. Thus, the effective exponent is given by

$$\rho_{eff}(h,L) = \ln \left[ \frac{M(2h,L) - M(+0)}{M(h,L) - M(+0)} \right] / \ln 2 , \qquad (87)$$

and the true value of the critical exponent  $\rho$  is obtained in the limit  $\rho = \lim_{h \to 0} \lim_{L \to \infty} \rho_{eff}(h, L)$ . As we see from Fig. 2, the effective exponent  $\rho_{eff}(h,L)$  increases monotoneously and converges to a certain value  $\rho_{eff}(h) = \lim_{L \to \infty} \rho_{eff}(h, L)$  with increasing of L. The data in Tab. 1  $\rho_{eff}(h, 2L) - \rho_{eff}(h, L)$ obey approximate scaling relation  $A\left[\rho_{eff}(4h,L)-\rho_{eff}(4h,L/2)\right]$  which holds with an almost constant value of coefficient A, i. e.,  $A \approx 1.15$  for L = 16 and  $A \approx 1.2$  for L = 32. According to the finite-size scaling theory  $L/\xi$  is the only essential scaling argument. It implies that the correlation length  $\xi$  is roughly proportional to  $h^{-1/2}$  within  $h \in [0.028; 0.64]$ . At h = 0.112 our results for L=32 closely agree with those at L=64, which indicates that  $\xi$  is several times smaller than 32 in this case. The actual scaling analysis then implies that  $\xi$  is several times smaller than L=64 at h=0.028. The scaling relation we found allows us to evaluate  $\rho_{eff}(h, 64) - \rho_{eff}(h)$  for  $h \ge 0.028$ . It leads to the conclusion that, with a high enough accuracy, our results at L=64 (solid circles in Fig. 2) correspond already to the

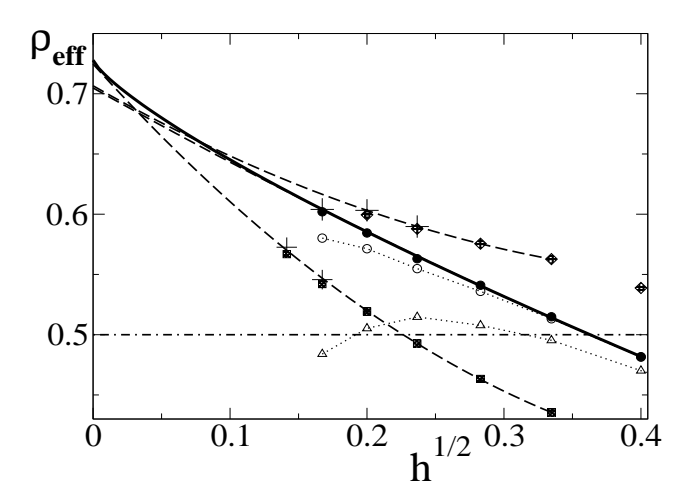


Figure 2: The effective exponent  $\rho_{eff}(h,L)$  for K=0.5 evaluated at L=16 (triangles), L=32 (empty circles), and L=64 (solid circles). The squares and rhombs show the L=64 results for two other couplings (temperatures) K=0.475 and K=0.55, respectively. The estimates for  $L=\infty$ , obtained by correcting the L=64 values, are swown by pluses. The statistical errors are within the symbol size. The dashed and solid lines show the fits  $\rho_{eff}(h)=\rho+a_1h^{1/2}+a_2h$  and  $\rho_{eff}(h)=\rho+ah^\omega$ , respectively. The horizontal dot–dashed line shows the asymptotic value of the "exact" RG theory.

thermodynamic limit at not too small fields  $h \ge 0.04$ , whereas a small correction (increment) about 0.002 is necessary to get the true value of  $\rho_{eff}(h)$  at h = 0.028. This value is indicated in Fig. 2 by a plus. Even larger than L = 64 lattices have to be considered for a reliable estimation of the thermodynamic limit at h = 0.02 an smaller fields.

According to the "exact" RG theory critised in Sec. 9.1, one can expect that  $\rho_{eff}(h)$  converges to the asymptotic value  $\rho=0.5$  linearly in  $h^{1/2}$  at  $h\to 0$ , as consistent with the expansion of M in powers of  $h^{1/2}$ . We have used this scale in Fig. 2 to show that the  $\rho_{eff}(h)$  vs  $h^{1/2}$  plot at K=0.5 (solid circles at h>0.28 and plus at h=0.28) goes, indeed, almost linearly, but clearly not to the "exact" value 0.5. Two different fits we made, namely,  $\rho_{eff}(h)=\rho+a_1h^{1/2}+a_2h$  (dashed curve) and  $\rho_{eff}(h)=\rho+ah^\omega$  (solid curve) yield  $\rho=0.705(9)$  and  $\rho=0.728(25)$  (with  $\omega=0.394(50)$ ), respectively. The fits of the first kind have been made also at K=0.475 and K=0.55 (lower and upper dashed lines) providing  $\rho=0.725(9)$  and  $\rho=0.707(36)$ , respectively. The fits of the second kind are not stable enough in these cases because of too large inaccuracy in  $\omega$ . The above listed estimates of  $\rho$  satisfactory well agree with the average value about 0.716 and, thus, confirm the expected universality of this exponent. A similar method of effective exponents has been tested in 2D Ising model [12] where it provided very accurate results.

The actual results for XY model agree with our prediction  $1/2 < \rho < 1$  for 3D case (cf. Sec. 9.6) and are incompatible with the conventional believe that  $\rho$  should be 1/2. To the contrary, it has been claimed in [38, 39] that the MC simulated magnetization data for O(4) and O(2) models well agree with the predictions of the Gaussian spin wave theory. However, we failed to see any serious argument in these papers by J. Engels et. al, since the only quantity which could be extracted from the magnetization data and precisely compared to the theory, i. e., the universal exponent  $\rho$ , has not been evaluated there. Moreover, their magnetization plots for the O(2) model are remarkably nonlinear

functions of  $h^{1/2}$ , i.e., they do not provide even an indirect evidence that  $\rho$  is just 1/2. The only values we found in [39], which can be compared to ours, are M(+0) = 0.5186(01)at K = 0.5 and M(+0) = 0.6303(1) at K = 0.55. Our respective values 0.519116(30)and 0.630545(24) are similar. Since there is no reason to assume that one of us has made a wrong simulation, the small but remarkable (5 their standard deviations at K=0.5) discrepancies, obviously, are due to the different extrapolation procedures used. Our values are more precise and reliable, since our method allows to estimate M(+0) from simulations at h=0 without any extrapolation over h used in [39]. Besides, we have used a larger maximal system size L=256 as compared to L=160 in [39]. As a result, the extrapolation gap in M is by an order of magnitude smaller in our case. The spontaneous magnetization M(+0) has been evaluated in [39] from the fit  $M(h) = M(+0) + ah^{\rho} + bh$  with  $\rho \equiv$ 1/2. In such away, the extrapolation which is biased by  $\rho = 1/2$  gives systematically underestimated values of M(+0) thus providing an indirect evidence that  $\rho \neq 1/2$ . If  $\rho = 1/2$  is replaced with  $\rho > 1/2$  in this ansatz, then the extrapolation gap becomes smaller (M(+0)) becomes larger) and the above discussed small discrepancies in M(+0)can be removed. This analysis suggests that  $\rho > 1/2$  holds, as consistent with the direct estimation in our paper.

#### 11 Conclusions

In the present work we have extended our diagrammatic method introduced in [5] to study the  $\varphi^4$  model in the ordered phase below the critical point, i. e., at  $T < T_c$ . In summary, we conclude the following.

- 1. The diagrammatic equations derived in [5] have been generalized to include the symmetry breaking term fixing the axis of ordering at  $T < T_c$  (Sec. 2).
- 2. An alternative formulation of our equations has been proposed. It has been shown that our equations coincide with the free energy variation principle (Sec. 3).
- 3. The solution for the two-point correlation (Greens) function depending on temperature T has been analyzed qualitatively not cutting the perturbation series. It includes the low-temperature solution at  $r_0 \to -\infty$  in the case of scalar order-parameter field (Sec. 7), as well as the general solution of n-component vector model at  $T \to T_c$  (Sec. 8).
- 4. Based on our diagrammatic equations, the asymptotic long-wave  $(k \to 0)$  behavior of the transverse and longitudinal Greens functions below  $T_c$  has been analyzed in Secs. 9.2 to 9.4. This analysis shows that  $G_{\perp}(\mathbf{k}) \simeq a \, k^{-\lambda_{\perp}}$  and  $G_{\parallel}(\mathbf{k}) \simeq b \, k^{-\lambda_{\parallel}}$  with exponents  $d/2 < \lambda_{\perp} < 2$  and  $\lambda_{\parallel} = 2\lambda_{\perp} d$ , and with universal ratio  $bM^2/a^2$  is the physical solution of our equations at the spatial dimensionality 2 < d < 4, which coincides with the asymptotic solution at  $T \to T_c$  as well as with the known rigorous results discussed in Sec. 9.1 and the non-pertubative renormalization group arguments provided in Sec. 9.5. It is confirmed also by the Monte Carlo simulations in Sec. 10. Formally, the results of the perturbative RG theory are recovered at  $\lambda_{\perp} = 2$ . However, we have disproven the conventional statement of this theory that  $\lambda_{\perp} = 2$  is the exact result (Sec. 9.1).

5. Monte Carlo simulations in 3D XY model has been performed (Sec. 10) to test the exponent  $\rho$ , describing the behavior of the magnetization  $M(h) - M(+0) \sim h^{\rho}$  in small external fields  $h \to 0$  below  $T_c$ . The simulation results confirm the universality of this exponent as well as our prediction  $1/2 < \rho < 1$ , and are incompatible with the value  $\rho = 1/2$  of the Gaussian spin wave theory supported by the perturbative RG analysis.

# **Appendix**

Here we study the thermodynamic limit of  $\Sigma(\mathbf{k},\zeta)$ , starting with  $\mathbf{k}=\mathbf{0}$ . For simplicity, we consider only the case of scalar order–parameter–field, i. e., n=1. The extension to the n-component case is trivial: the fixed zero–vectors always refer to the longitudinal component. According to the definition of  $\Sigma(\mathbf{0},\zeta)$  (cf. Eqs. (11) to (14)), this quantity obeys a selfconsistent diagrammatic equation

$$\Sigma(\mathbf{0},\zeta) \simeq \begin{array}{c} \mathbf{0} \\ \mathbf{0} \end{array} + \begin{array}{c} \mathbf{0} \\ \mathbf{0} \end{array} + \begin{array}{c} \mathbf{0} \\ \mathbf{0} \end{array}$$
 (A1)

where the block represents a resummed perturbation series of all connected diagrams of this kind, which do not contain parts like and/or and/or and cannot be split in two as follows . At  $\zeta = 1$ , all connected diagrams with four fixed outer lines and vectors  $\mathbf{k}_1$ ,  $\mathbf{k}_2$ ,  $\mathbf{k}_3$ ,  $\mathbf{k}_4 = -\mathbf{k}_1 - \mathbf{k}_2 - \mathbf{k}_3$  represent the perturbation sum of the cumulant four-point correlation function

$$G_c(\mathbf{k}_1, \mathbf{k}_2, \mathbf{k}_3) = G(\mathbf{k}_1, \mathbf{k}_2, \mathbf{k}_3)$$

$$-G(\mathbf{k}_1, \mathbf{k}_2) G(\mathbf{k}_3, \mathbf{k}_4) - G(\mathbf{k}_1, \mathbf{k}_3) G(\mathbf{k}_2, \mathbf{k}_4) - G(\mathbf{k}_1, \mathbf{k}_4) G(\mathbf{k}_2, \mathbf{k}_3)$$
(A2)

where  $G(\mathbf{k}_1, \mathbf{k}_2) \equiv \delta_{\mathbf{k}_1, -\mathbf{k}_2} G(\mathbf{k}_1)$  is the two-point correlation function. In principle, the diagrams of  $G_c(\mathbf{k}_1, \mathbf{k}_2, \mathbf{k}_3)$  can be grouped like those of  $\Sigma(\mathbf{k}, \zeta)$  following [5]. It implies the summation over the chains of blocks —, yielding skeleton diagrams with respect to the solid lines, followed by the summation over the chains of blocks ——, yielding skeleton diagrams with respect to the waved lines. We remind that the skeleton diagrams are those connected diagrams where the true correlation function  $G(\mathbf{k})$  is related to the solid lines and the dashed lines inside the diagrams are replaced by the waved lines. Besides, the skeleton diagrams do not contain parts — and  $\infty$  . In such a way, the perturbation sum of  $G_c(\mathbf{0},\mathbf{0},\mathbf{0})$  is almost the same as 0 with the only difference that it includes also the diagrams like 0 with the equation for  $G_c(\mathbf{0},\mathbf{0},\mathbf{0})$ ,

$$G_c(\mathbf{0}, \mathbf{0}, \mathbf{0}) = \begin{array}{cccc} \mathbf{0} & \mathbf{0$$

in which the diagram blocks are calculated at  $\zeta = 1$ . In analogy to  $G(\mathbf{0}) \simeq M^2V$  (cf. eq. (23)), the zero-vector term  $V^{-2}G(\mathbf{0},\mathbf{0},\mathbf{0})$  represents the constant (non-decaying) contribution  $M^4$  to the real-space four-point correlation function below  $T_c$ . According to (A2), it means that

$$G_c(\mathbf{0}, \mathbf{0}, \mathbf{0}) = -2M^4V^2$$
 at  $V \to \infty$ . (A4)

At the first step we take into account only those contributions where  $\mathbf{k} = \mathbf{0}$  vectors are related to the connecting solid lines inside the last diagram in (A3). Then, together with (A4), (A1), and (12), we have a system of selfconsistent equations yielding

$$\Sigma(\mathbf{0}, 1) \propto V \tag{A5}$$

with two possible values of the proportionality factor  $-\left(5 \pm \sqrt{17}\right) u M^4$ . One of possibilities is that the additional terms with non–zero wave vectors related to the connecting solid lines in (A3) give a negligible corretion at  $V \to \infty$ , as consistent with the following idea. The four–point function  $G(\mathbf{k}, -\mathbf{k}, \mathbf{0})$  behaves like  $M^2VG(\mathbf{k})$  below  $T_c$ , as it follows from a simple consideration of the limit where two points of the real–space four–point correlation function are infinitely distant. However, this term cancellates in the cumulant average  $G_c(\mathbf{k}, -\mathbf{k}, \mathbf{0})$  at  $\mathbf{k} \neq \mathbf{0}$  entering the equation, analogous to (A3), for the block  $\mathbf{k} = \mathbf{0}$ 

-k  $\longrightarrow$  0 . As a result, a selfconsistent solution exists where this block is vanishingly small as compared to V and Eq. (A5) remains correct. Nevertheless, other kind of selfconsistent solutions cannot be excluded where all terms on the right-hand side of Eq. (A3)

and of similar equations for the blocks  ${}^{\mathbf{k}}_{-\mathbf{k}} = {}^{\mathbf{0}}_{\mathbf{0}}$  and  ${}^{\mathbf{k}}_{-\mathbf{k}} = {}^{\mathbf{q}}_{-\mathbf{q}}$  are compatible. The latter is possible if the block in (A3), having four fixed zero–vectors, diverges as  $V^{2+\mu}$  with  $\mu \geq 0$ , whereas the above mentioned blocks with non–zero vectors  $\mathbf{k}$  and  $\mathbf{q}$  diverge like  $V^{1+\mu}$  and  $V^{\mu}$ , respectively. In this case  $\Sigma(\mathbf{0},1)$  is proportional to  $V^{1+\mu}$ .

Contrary to the case of  $\mathbf{k} = \mathbf{0}$ , the thermodynamic limit exists for the function  $\Sigma(\mathbf{k}, 1)$  at  $\mathbf{k} \neq \mathbf{0}$ , as it can be found easily by a suitable grouping of the divergent terms in (11). Only those terms can diverge at  $V \to \infty$  which contain insertions with 2m outer solid

zero-vector lines, like  $0 \longrightarrow 0$ ,  $0 \longrightarrow 0$ , etc. In an ordinary case m factors  $G(\mathbf{0}) \simeq M^2V$  related to m solid lines with fixed  $\mathbf{k} = \mathbf{0}$  vectors are compensated by a removal of m integrations over wave vectors, as consistent with the well known rule  $\sum_{\mathbf{k}} \to V(2\pi)^{-d} \int d\mathbf{k}$ . This condition is violated if the constraints  $\mathbf{k} = \mathbf{0}$  are not independent. The sum of all wave vectors coming out from any node is zero. As a consequence, this property holds also for any block. Therefore only 2m-1 constraints  $\mathbf{k} = \mathbf{0}$  for 2m outer solid lines of the above discussed insertions are independent, i. e., only 2m-1 integrations are removed. As a result, any such insertion provides a diverging factor  $\propto V$  for the resulting diagram unless this factor is compensated by vanishing waved line with fixed  $\mathbf{k} = \mathbf{0}$ . Due to these properties, the constraints  $\mathbf{k} = \mathbf{0}$  for 2m solid lines connecting two parts of a diagram like  $0 \longrightarrow 0$  also are not independent, but this situation

Thus, some diagrams containing specific insertions with 2m outer zero-vector solid lines are divergent. At the same time, all such insertions with 2m outer lines represent the perturbation sum of the 2m-point cumulant correlation function with all zero arguments. In general, the 2m-point cumulant  $G_c^{(2m)}(\mathbf{k}_1, \mathbf{k}_2, \dots, \mathbf{k}_{2m-1})$  is defined as

is possible only for the diagrams of  $\Sigma(\mathbf{0}, \zeta)$ .

$$G_c^{(2m)}(\mathbf{k}_1, \mathbf{k}_2, \dots, \mathbf{k}_{2m-1}) = G^{(2m)}(\mathbf{k}_1, \mathbf{k}_2, \dots, \mathbf{k}_{2m-1}) - S^{(2m)}(\mathbf{k}_1, \mathbf{k}_2, \dots, \mathbf{k}_{2m-1}), (A6)$$

where  $G_c^{(2m)}$  is given by resummed connected diagrams, i. e., a diagram block with 2m fixed outer solid lines, whereas  $S^{(2m)}$  represents the sum over all possible splitings of this block in smaller parts. These functions contain only 2m-1 independent arguments (wave

vectors of outer solid lines), since the sum over all 2m wave vectors is zero. The correlation function  $G^{(2m)}\left(\mathbf{0},\mathbf{0},\ldots,\mathbf{0}\right)$  is related to the non-decaying part  $M^{2m}$  of the real-space 2m-point correlation function and, thus (according to the Fourier transformation), is  $M^{2m}V^m$  at  $V\to\infty$ . From (A6) we find that  $G_c^{(2m)}\left(\mathbf{0},\mathbf{0},\ldots,\mathbf{0}\right)$  is proportional to  $M^{2m}V^m$ . In such a way, we can resummate the specific zero-vector insertions to replace the perturbation sums by corresponding 2m-point cumulants. It is then straightforward to see that any inserted 2m-point zero-vector cumulant does not cause a divergence at  $V\to\infty$ , but only renormalize the original diagram by a constant factor. Namely, m solid zero-vector lines of the original diagram are broken to insert the cumulant block, thus replacing the previous factor  $[G(\mathbf{0})]^m \simeq M^{2m}V^m$  of these zero-vector lines with the cumulant value  $Q_m M^{2m}V^m$ , where  $Q_m$  is a constant.

Not only the function  $\Sigma(\mathbf{k},\zeta)$ , but also the derivative  $\partial \Sigma(\mathbf{q},\zeta)/\partial G(\mathbf{k})$  is relevant to our analysis. This derivative is represented by diagrams obtained by breaking one solid line with wave vector  $\mathbf{k}$  in the diagrams of  $\Sigma(\mathbf{q},\zeta)$ , removing the corresponding factor  $G(\mathbf{k})$ . Let us consider those diagrams of  $\partial \Sigma(\mathbf{q},1)/\partial G(\mathbf{k})$  with  $\mathbf{k} \neq \mathbf{0}$ , containing the zero–vector–cumulant insertions, where the broken solid line does not belong to any of the inserted blocks. The diagrams including resummed blocks of this kind and the corresponding "normal" diagrams whith no insertions differ merely by constant factors. Namely, as in the case of  $\Sigma(\mathbf{k},1)$ , any insertion of a resummed 2m–point cumulant block with 2m outer zero–vector lines gives a constant factor  $Q_m$  at  $V \to \infty$ .

Below we prove that the derivative  $\partial Q_m/\partial G(\mathbf{k})$  vanishes at  $V\to\infty$ . As a result, the corresponding terms where solid line is broken inside a zero–vector–cumulant block do not give an extra contribution to  $\partial \Sigma(\mathbf{q},1)/\partial G(\mathbf{k})$ . Quantity  $M^{2m}V^m\partial Q_m/\partial G(\mathbf{k})$ , is represented by the skeleton diagrams of  $G_c^{(2m)}(\mathbf{0},\mathbf{0},\ldots,\mathbf{0})$  in which one solid line with vector  $\mathbf{k}$  is broken in two, removing the factor  $G(\mathbf{k})$ . If factors  $G(\mathbf{k})$  and  $G(-\mathbf{k})\equiv G(\mathbf{k})$  are restored for both parts of the broken line, we obtain the diagrams of  $G_c^{(2m+2)}(\mathbf{k},-\mathbf{k},\mathbf{0},\ldots,\mathbf{0})$ . To simplify the further notation we shall replace the above set of arguments with one argument  $\mathbf{k}$ . Thus, a resummation of these diagrams yields

$$M^{2m}V^m \left[ G(\mathbf{k}) \right]^2 \partial Q_m / \partial G(\mathbf{k}) = G_c^{(2m+2)}(\mathbf{k}) . \tag{A7}$$

According to the physical arguments we have

$$G^{(2m)}(\mathbf{0}) = M^{2m}V^m \,, \tag{A8}$$

$$G^{(2m+2)}(\mathbf{k}) = G(\mathbf{k}) M^{2m} V^m$$
 (A9)

at  $V \to \infty$ . Eq. (A8) represents the condition for the non-decaying part  $M^{2m}V^m$  of the 2m-point real-space correlation function, whereas (A9) describes the limit where 2m points of the (2m+2)-point function are infinitely distant. By setting m=2 in (A6) and taking into account (A9), we obtain at  $\mathbf{k} \neq \mathbf{0}$ 

$$M^{-2}V^{-1}G_c^{(4)}(\mathbf{k}) = G(\mathbf{k}) - G(\mathbf{k})G(\mathbf{0})M^{-2}V^{-1} = 0$$
 at  $V \to \infty$ . (A10)

We can prove by induction over  $\ell$  that  $M^{-2\ell}V^{-\ell}G_c^{(2\ell+2)}(\mathbf{k}) = 0$  holds at  $V \to \infty$  for any  $\ell \ge 1$  and  $\mathbf{k} \ne \mathbf{0}$ . Eq. (A10) means that it holds at  $\ell = 1$ . If it holds for  $\ell < m$ , then the only relevant terms in the equation (A6) for the (2m+2)-point cumulant are

$$G_c^{(2m+2)}(\mathbf{k}) = G^{(2m+2)}(\mathbf{k}) - G(\mathbf{k}) G_c^{(2m)}(\mathbf{0}) - G(\mathbf{k}) S^{(2m)}(\mathbf{0}),$$
 (A11)

which yield vanishing result for  $M^{-2m}V^{-m}G_c^{(2m+2)}(\mathbf{k})$  according to Eq. (A6) for zero-vector cumulants, as well as (A8) and (A9). According to (A7), the latter means that quantity  $\partial Q_m/\partial G(\mathbf{k})$  vanishes (at  $\mathbf{k} \neq \mathbf{0}$ ) in the thermodynamic limit  $V \to \infty$ .

However, if it would not vanish, then it would produce a contribution to the derivative  $\partial \Sigma(\mathbf{q},1)/\partial G(\mathbf{k})$  which is by a factor V larger than the ordinary terms  $\sim V^{-1}$ . It means that not only the leading behavior, but also the corrections to finite–size scaling in (A8) and (A9) could play some role. At n=1 these corrections are exponentially small, as consistent with the known exponential decay of the real–space correlation functions in Ising model below  $T_c$ . The latter is true also at n>1 for the longitudinal component of the correlation functions at finite values of the amplitude  $\delta$  of the symmetry–breaking term in (3), since in this case Hamiltonian (3) looses the rotational symmetry and, therefore, belongs to the Ising universality class. Since  $\delta$  is a continuous parameter, the exponential decay of correlations will be observed at large enough distances x for any arbitrarily small, but finite value of  $\delta$ . It means that the corrections are exponentially small in our limit  $\lim_{\delta \to 0} \lim_{L \to \infty} t$ , where L is the linear size of the system. There is no any contradiction with the power–like decay of correlations we found at n>1, since this decay refers to the limit where  $x\to\infty$  and, simultaneously,  $x/L\to0$  hold (i. e., we find the thermodynamic limit at any given nonzero wave vector).

Thus, we finally arrive to the conclusion that corrections to (A8) and (A9) are exponentially small in  $L=V^{1/d}$  and, therefore,  $\partial Q_m/\partial G(\mathbf{k})=0$  holds at  $\mathbf{k}\neq\mathbf{0}$  with a high enough accuracy, i. e., quantities  $Q_m$  can be treated as pure constants providing no extra contributions due to their variations. As discussed before, it means that the inserted zero-vector-cumulants merely renormalize by constant factors the "normal" terms in the diagram expansion of  $\Sigma(\mathbf{k},1)$  and  $\partial \Sigma(\mathbf{q},1)/\partial G(\mathbf{k})$ . Since our analysis is not based on specific values of expansion coefficients, this renormalization cannot affect our qualitative conclusions. It means that the general scaling form of  $\Sigma(\mathbf{k},1)$  and  $\partial \Sigma(\mathbf{q},1)/\partial G(\mathbf{k})$  is correctly predicted by the simplified analysis which ignores the zero-vector-cumulant insertions.

Our foregoing consideration of  $\Sigma(\mathbf{k},\zeta)$  is restricted to  $\zeta=1$  due to a technical reason that the relation to cumulant correlation functions with a certain physical meaning is known only for this case. Since  $\zeta$  is a continuous parameter, we believe that the above discussed properties remain true for all values of interest, i. e.,  $\zeta \in [0; 1]$ .

We can use the alternative method to find quantity  $R_i(\mathbf{k})$ , as proposed in Sec. 3. It is straightforward to check in each specific case we considered in our paper that Eq. (17) provides the same scaling properties of  $R_i(\mathbf{k})$  at  $\mathbf{k} \neq \mathbf{0}$  as the equations (8) and (39). Regarding the "normal" terms, it is easy to verify (like in Secs. 9.2-9.3 and in Sec. 7) that in the most nontrivial case of n > 1 at  $k \to 0$  below  $T_c$ , as well as at  $r_0 \to -\infty$  in the case of n = 1, the main contribution comes from all diagrams of Eq. (17) in which the waved lines have nonzero wave vectors and each second solid line with i = 1 has fixed wave vector  $\mathbf{k} = \mathbf{0}$  (i. e., there are no integrations in the case of n = 1), counting the pair of outer lines as one line. This peculiarity does not refer to the case  $T \to T_c$ , where all the partial contributions with  $M^0$ ,  $M^2$ ,  $M^4$ , etc., are compatible. The two different modifications of our method obviously give consistent corrections to scaling: they have the same origin. The alternative approach [Eq. (17)] does not suffer from the problems with parameter  $\zeta < 1$ , since we have  $\zeta \equiv 1$ . As before, the zero-vector-cumulant insertions merely renormalize by constant factors the "normal" terms. It proves the statement that

the simplified analysis, ignoring these insertions, provides correct general scaling form of the solution for  $R_i(\mathbf{k})$  and, therefore,  $G_i(\mathbf{k})$ .

## Acknowledgements

The Monte Carlo simulations have been made and the results have been discussed during my stay at the Physics Department of Rostock University, Germany.

# References

- [1] D. Sornette, Critical Phenomena in Natural Sciences, Springer, Berlin, 2000
- [2] J. G. Brankov, D. M. Danchev, N. S. Tonchev, Theory of Critical Phenomena in Finite-Size Systems: Scaling and Quantum Effects, World Scientific, 2000
- [3] Shang–Keng Ma, Modern Theory of Critical Phenomena, W.A. Benjamin, Inc., New York, 1976
- [4] J. Zinn-Justin, Quantum Field Theory and Critical Phenomena, Clarendon Press, Oxford, 1996
- [5] J. Kaupužs, Ann. Phys. (Leipzig) **10** (2001) 299
- [6] L. Onsager, Phys. Rev. **65** (1944) 117
- [7] Rodney J. Baxter, Exactly Solved Models in Statistical Mechanics, Academic Press, London, 1989
- [8] N. Ito, M. Suzuki, Progress of Theoretical Physics, 77 (1987) 1391
- [9] N. Schultka, E. Manousakis, Phys. Rev. B **52** (1995) 7258
- [10] L. S. Goldner, G. Ahlers, Phys. Rev. B 45 (1992) 13129
- [11] J. Kaupužs, e-print cond-mat/0201221
- [12] J. Kaupužs, e-print cond-mat/0405197
- [13] A. Z. Patashinskii, V. L. Pokrovskii, Zh. Eksp. Teor. Fiz. 64 (1973) 1445
- [14] F. Schwabl, K. H. Michel, Phys. Rev. B 2 (1970) 189
- [15] H. Wagner, Z. Phys., **195** (1966) 273
- [16] F. J. Dyson, Phys. Rev., **102** (1956) 1217; 1230
- [17] M. E. Fisher, M. N. Barber, D. Jasnow, Phys. Rev. A. 8 (1973) 1111
- [18] E. Brezin, D. J. Wallace, Phys. Rev. B 7 (1973) 1967
- [19] D. J. Wallace, R. K. P. Zia, Phys. Rev. B 12 (1975) 5340
- [20] D. R. Nelson, Phys. Rev. B **13** (1976) 2222

- [21] E. Brezin, J. Zinn-Justin, Phys. Rev. B 14 (1976) 3110
- [22] L. Schaefer, H. Horner, Z. Phys. B **29** (1978) 251
- [23] I. D. Lawrie, J. Phys. A **14** (1981) 2489
- [24] I. D. Lawrie, J. Phys. A **18** (1985) 1141
- [25] U. C. Tuber, F. Schwabl, Phys. Rev. B 46 (1992) 3337
- [26] I. Madzhulis, J. Kaupužs, Phys. Stat. Sol. (b) 175 (1993) 307
- [27] J. Goldstone, Nuovo Cimento **19** (1961) 154
- [28] P. Hasenfratz, H. Leutwyler, Nucl. Phys. **B343** (1990) 241
- [29] T. Koma, H. Tasaki, Phys. Rev. Lett. **74** (1995) 3916
- [30] J. Fröhlich, T. H. Spencer, Comm. Math. Phys. 81 (1981) 527
- [31] H. E. Boos, V. E. Korepin, Y. Nishiyama, M. Shiroishi, J. Phys. A 35 (2002) 4443
- [32] I. Dimitrović, P. Hasenfratz, J. Nager, F. Niedermayer, Nucl. Phys. B350 (1991) 893
- [33] S. Tominaga, H. Yoneyama, Phys. Rev. **B51** (1995) 8243
- [34] N. Stüsser, M. Rekveldt, T. Spruijt, Phys. Rev. B 33 (1986) 6423
- [35] U. Wolff, Phys. Rev. Lett. **62** (1989) 361
- [36] M. E. J. Newman, G. T. Barkema, Monte Carlo Methods in Statistical Physics, Clarendon Press, Oxford, 1999
- [37] W. H. Press, B. P. Flannery, S. A. Teukolsky, W. T. Vetterling, Numerical Recipes The Art of Scientific Computing, Cambridge University Press, Cambridge, 1989
- [38] J. Engels, T. Mendes, Nucl. Phys. B **572** (2000) 289
- [39] J. Engels, S. Holtman, T. Mendes, T. Schulze, Phys. Lett. B 492 (2000) 492